

**Studies on the Physiology and Glucose Metabolism of 14-16-Month-Old
Female RTSKO Mice**

by

Kalsha Hansini Diagarachchige De Silva

A thesis

presented to the University of Waterloo

in fulfillment of the

thesis requirement for the degree of

Master of Science

in

Kinesiology

Waterloo, Ontario, Canada, 2020

© Kalsha Hansini Diagarachchige De Silva 2020

Author's Declaration

I hereby declare that I am the sole author of this thesis. This is a true copy of the thesis, including any required final revisions, as accepted by my examiners.

I understand that my thesis may be made electronically available to the public.

Abstract

Obesity is a global epidemic. Characterized by an imbalance between energy intake and expenditure, the metabolic and physiological dysfunctions that it yields can result in other diseases such as diabetes. Although several factors play a role, ectopic lipid accumulation in organs such as the liver, heart and skeletal muscle has been found to be an intermediary between obesity and related comorbidities. However, the specific role of lipid accumulation in the kidney remains unpublished, since isolated models of renal steatosis are absent from the literature. The Lipid Enzyme Discovery lab has generated a novel murine model of renal steatosis, where the first exon of the *Pnpla2* gene encoding adipose triglyceride lipase has been deleted in the epithelial cells of the proximal and distal renal tubules, impairing lipolysis. In prior work by our laboratory, characterization of Renal Tubule-Specific *Adipose Triglyceride Lipase* Knockout (RTSAKO) mice has demonstrated a significant sexual dimorphism, wherein young male mice develop glucose intolerance by 16-18-weeks of age, that is absent in young female mice (manuscript in preparation). Notably, those males do not have impaired insulin sensitivity, but do have decreased circulating insulin concentrations, suggesting impaired insulin secretion. In humans, females often develop the same chronic diseases as males, but with a longer latency. My work extends our laboratory's initial findings in young mice, by studying female RTSAKO mice and their control littermates at 14-16 months. Phenotypic characterization of this murine model indicated that body weights, adipose tissue weights, and the weights of most organs were not different between RTSAKO mice and littermate controls, but kidney weights were increased, suggesting the development of renal steatosis. Notably, this was not accompanied by evidence of kidney lipotoxicity or inflammation, since there were no changes in the renal gene expression of various biomarkers of inflammation, fibrosis and proliferation. Similar to the younger male mice,

female RTSAKO mice aged 14-16 months were glucose intolerant, but insulin sensitive. They also had lower serum insulin concentrations as determined using Bio-plex analysis. Prior work completed by our laboratory has implicated the bioactive lipid, lysophosphatidic acid (LPA), in impairing insulin secretion in young male RTSAKO mice. Therefore, acute treatment with Ki16425, an LPA receptor 1 and 3 inhibitor, was tested and found to restore glucose tolerance in 14-16-month-old female RTSAKO mice, providing evidence that this lipid is also mechanistically implicated in impairing glycemic control in the aged female mice. Because bioactive LPA can affect behavior, studies on activity and energy expenditure were performed using metabolic chambers. While these showed no significant differences between the RTSAKO mice and control littermates, the aged female RTSAKO mice did appear to have lower activity patterns overall, suggesting the results may have been underpowered, and that a larger cohort may aid in elucidating potential differences. Therefore, this thesis investigates the metabolic and physiological changes in female RTSAKO mice at a defined age of 14-16 months.

Acknowledgements

Dr. Robin E. Duncan

I would like to thank Dr. Robin E. Duncan my supervisor for her selfless support throughout the years. She has immensely cared for my mental and emotionally wellbeing when the pressures of grad school sometimes became too overwhelming. To joking refer to her as a “mother away from home” is not an overstatement, as her kind-natured personality has made my master’s experience an educational, informational and a memorable one. I am forever grateful and thankful for her!

Dr. Maria Fernanda Fernandes

Thank you to Dr. Fernandes, a Post-Doctoral Fellow in our lab. She took me on and has mentored me since day one. I’ll always remember the knowledge that she has given me.

Ash, John, Joey & Michelle

I sincerely thank you all for always being there and making my time a truly memorable one. Each and every one of you has helped in many ways, either its going through a protocol (Ash), letting me use your reagents (Joey), showing me how to use a software (John) or simply lending an ear to listen to my sorrows (Michelle). Over the year, we have become an inseparable work family which I truly treasure at heart and hope that it will forever stays that way!

My Parents

Your unconditional love, care and support has made me the person I am today. Thank you for always supporting and believing in me through the tough times. Moving to a new country 15 years ago was a new journey we all embarked on, but I am happy to look back and say that we are almost there! It means the world to me to have you both by my side cheering me on forever. Thank you Ammi and Thati!

To My Loving Parents

DMSD.

Table of Contents

<i>Author's Declaration</i>	<i>ii</i>
<i>Abstract</i>	<i>iii</i>
<i>Acknowledgements</i>	<i>v</i>
<i>Dedication</i>	<i>vi</i>
<i>List of Figures</i>	<i>ix</i>
<i>List of Tables</i>	<i>x</i>
<i>List of Abbreviations</i>	<i>xi</i>
Chapter 1: Introduction	1
<i>Obesity, Diabetes, and Ectopic Lipid Accumulation</i>	1
<i>The Role of Kidney in Blood Glucose Regulation</i>	4
<i>Renal Lipid Accumulation</i>	6
<i>Age Related Changes in Female Health</i>	7
<i>An Appropriate Mouse Model</i>	8
<i>Present Research Interests</i>	10
Chapter 2: Biochemical Foundations	12
<i>Introduction</i>	12
<i>Lipolysis</i>	12
<i>Adipose Triglyceride Lipase</i>	13
<i>Hormone-Sensitive Lipase</i>	14
<i>Monoglyceride Lipase</i>	15
<i>Lysophosphatidic Acid</i>	15
<i>Insulin</i>	18
<i>Glucagon</i>	19
<i>Leptin</i>	20
<i>Resistin</i>	20
Chapter 3: Phenotypic Characterization and Renal Expression of Select Genes Involved in Lipolysis, Lipogenesis, Inflammation, Fibrosis, and Proliferation in the 14-16-Month-Old Female RTSAKO Mice	22
<i>Rationale:</i>	22
<i>Objectives:</i>	24
<i>Hypotheses:</i>	24
<i>Methods:</i>	26
<i>Study Design</i>	26

<i>RTSAKO Knockout Mouse Model</i>	26
<i>DNA Isolation</i>	28
<i>Genotyping</i>	28
<i>RNA Extraction</i>	29
<i>Real-Time Polymerase Chain Reaction (RT-PCR) and CDNA synthesis</i>	29
<i>Quantitative PCR (qPCR)</i>	30
<i>Mice Used</i>	33
<i>Statistical Analysis</i>	33
Results:	34
Discussion:	41
Chapter 4: Studies on Glucose Tolerance and Insulin Sensitivity in 14-16-Month-Old Female RTSAKO Mice	45
Rationale:	45
Objectives:	46
Hypotheses:	46
Methods:	47
<i>Study Design</i>	47
<i>Glucose Tolerance Test</i>	47
<i>Insulin Tolerance Test</i>	47
<i>Ki16425 Injection</i>	48
<i>Bio-plex – Hormonal analysis</i>	48
<i>Mice Used</i>	49
Statistical Analysis	50
Results:	51
Discussion:	58
Chapter 5: Measures of Activity and Energy Expenditure in 14-16-month-old Female RTSAKO mice	61
Rationale:	61
Objective:	62
Hypotheses:	62
Methods:	63
<i>Comprehensive Lab Animal Monitor System (CLAMS)</i>	63
<i>Food Composition</i>	63
<i>Mice Used</i>	64
<i>Statistical Analysis</i>	64
Results:	65
Discussion:	74
Chapter 6: Integrated Conclusion	76
References	83

List of Figures

- Figure 1: Breeding strategy for the RTSAKO and Control Mice
Figure 2: Expression of Cre-Recombinase
Figure 3: Body and Organs Weights of Control (CT) and Knockout (RTSAKO) mice
Figure 4: Renal expression of *Hsl*, *Dgat1*, and *Lipin 1*
Figure 5: Expression of Genes Implicated in Inflammation in Kidneys of Control (CT) and Knockout (RTSAKO) mice
Figure 6: Expression of Genes Implicated in Fibrosis
Figure 7: Expression of Proliferation Regulation Genes
Figure 8: Glucose Tolerance Testing in Control (CT) and Knockout (RTSAKO) mice
Figure 9: Insulin Tolerance Testing in Control (CT) and Knockout (RTSAKO) mice
Figure 10: Glucose tolerance of RTSAKO mice and control (CT) littermates following Ki16425 Pre-treatment
Figure 11: Food-intake and Body weight in Control (CT) and Knockout (RTSAKO) mice
Figure 12: Activity During the Day and Night in Control (CT) and Knockout (RTSAKO) mice
Figure 13: Oxygen consumption rate of Control (CT) and Knockout (RTSAKO) mice
Figure 14: Volume of Carbon Dioxide (VCO₂) in Control (CT) and Knockout (RTSAKO) mice
Figure 15: RER and Heat in Control (CT) and Knockout (RTSAKO) mice

List of Tables

- Table 1: Primers for Housekeeping Genes
- Table 2: Primers for Genes Implicated in Inflammation
- Table 3: Primers for Genes Implicated in Fibrosis
- Table 4: Primers for Genes Implicated in Lipogenesis
- Table 5: Primers for Genes Implicated in Lipolysis
- Table 6: Primers for Genes Implicated in Proliferation
- Table 7: Bio-plex Hormone Assay

List of Abbreviations

BMI – Body Mass Index
CKD – Chronic Kidney Disease
CVD – Cardiovascular Disease
DM – Diabetes Mellitus
T1DM – Type 1 Diabetes
T2DM – Type 2 Diabetes
ER – Endoplasmic Reticulum
NEFA – Nonesterified Fatty Acids
TAG – Triacylglycerol
DAG – Diacylglycerol
FOXO – Forkhead Box O
GLUT – Glucose Transporter
SGLT – Sodium-coupled glucose transporter
ATGL – Adipose Triglyceride Lipase
NAFLD – Non-alcoholic fatty liver disease
VCD – 4-vinylcyclohexene diepoxide
RTSAKO – Renal Tubule Specific Adipose Triglyceride Lipase Knockout
CT – Control
LPA – Lysophosphatidic Acid
HSL – Hormone Sensitive Lipase
MAG – Monoacylglycerol
MGL – Monoglyceride Lipase
Pnpla2 – Patatin-like phospholipase domain containing protein 2
WAT – White adipose tissue
BAT – Brown adipose tissue
cAMP – Cyclic adenosine monophosphate
PKA – Protein kinase A
GPCR – G protein-coupled receptor
PA – Phosphatidic acid
GIP – Gastric inhibitory polypeptide
GIPR – Gastric inhibitory polypeptide receptor
DPP-4 – Dipeptidyl peptidase-4
PAI-1 – Plasminogen Activator Inhibitor-1
TNF α – Tumor necrosis factor- α
FFA – Free Fatty Acid
GTT – Glucose Tolerance testing
ITT – Insulin tolerance testing
DGK ϵ – Diacylglycerol Kinase Epsilon
DGAT-1 – Diacylglycerol O-acyltransferase 1
IL-1 β – Interleukin 1 beta
IL-6 – Interleukin-6
COL1A1 – Collagen type 1 alpha 1
COL4A1 – Collagen type 4 alpha 1
FN-1 – Fibronectin 1

PCNA – Proliferating cell nuclear antigen
AGK – Acylglycerol Kinase
VO₂ – Volume of oxygen
VCO₂ – Volume of carbon dioxide
RER – Respiratory exchange ratio
CLAMS – Comprehensive Lab Animal Monitor System

Chapter 1: Introduction

Obesity, Diabetes, and Ectopic Lipid Accumulation

Obesity, a rising epidemic, is expected to affect nearly 20% of the world's population by 2030 [1]. Individuals are categorized as “obese” when body mass index (BMI), which is obtained using body weight and height, exceed a value of 30 kg/m² [1, 2]. The excess adiposity arises primarily due to an energy imbalance, where caloric intake outweighs expenditure [1]. This chronic surplus of energy, in combination with various other individual factors such as genetics and lifestyle choices, drive this disease [1]. The resulting positive energy balance is key in causing an accumulation of fat in both adipose and non-adipose tissues in individuals with obesity [1, 3]. In addition to BMI, waist circumference is used clinically as an indication of a more dangerous type of adiposity due to the presence of visceral fat [1]. Obesity shortens life expectancy by 4-7 years, since the risk of mortality from co-morbid diseases, such as diabetes, chronic kidney disease (CKD) and cardiovascular disease (CVD), is significantly raised [1-4].

Diabetes mellitus (DM) is a metabolic disease characterized by elevated blood glucose levels resulting from deficits in insulin secretion [5, 6]. Depending on the deficiency of insulin, an individual can be categorized as either a type 1 (T1DM) or type 2 (T2DM) diabetic [5]. T1DM can be fulminant, idiopathic or autoimmune, although the latter is the most prominent subtype [5]. Autoimmune type 1 diabetes is commonly first diagnosed in children and adolescents [6]. Here, the β cells of the pancreas are damaged due to an inflammatory response mediated by the B and T cells of the body [6]. Therefore, in type 1 diabetes there is a partial or complete insufficiency in insulin production, and individuals are dependent on exogenous insulin to correct postprandial hyperglycemia [7]. Although T1DM was the major form in the first half

of the 20th century, T2DM has risen in prevalence to become a global epidemic, and currently more than 90% of diabetic patients are categorized as such [6].

Hyperglycemia in T2DM is characterized by a relative insulin deficiency, where resistance to the action of insulin has increased the level of insulin that is required to mediate glucose disposal [6, 7]. When insulin output by the pancreas becomes insufficient to mediate glucose disposal in the face of worsening insulin resistance, fasting hyperglycemia and T2DM results [6]. T2DM patients are not always insulin dependent, particularly in early stages, since glucose levels can often be controlled by drugs that improve insulin secretion or function, or by dietary and lifestyle changes that improve peripheral tissue and hepatic insulin sensitivity, thereby reducing insulin requirements [8]. However, if changes are not implemented to lower demands on the pancreas for insulin production, then over time the excessive demand for synthesis of insulin peptide hormone by the endoplasmic reticulum (ER) results in oxidative stress, which causes the gradual loss of β cells in a phenomenon termed β cell exhaustion [9, 10]. This transition from relative insufficiency to absolute deficiency in insulin-producing cells can cause T2DM patients to become insulin-dependent, and therefore more characteristic of T1DM patients [5, 6].

Obesity is a major risk factor for the development of T2DM, and obese individuals are seven times more likely to develop T2DM than individuals with a normal body mass [1, 2, 6]. Obesity is associated with an increase in circulating cytokines, nonesterified fatty acids (NEFA), and other bioactive lipids and hormones, which mechanistically link obesity to the development of insulin resistance [11-13]. Obesity is also associated with the dysregulation of lipid storage, and with abnormal elevations in triacylglycerol (TAG) and other lipids in various organs [14,

15]. Ectopic lipid accumulation refers to the abnormal accretion of lipid droplets in non-adipose tissues [15].

In obesity, an elevated and continuous supply of circulating NEFA can occur. Normally, insulin would suppress the post-prandial release of NEFA, but this action is impaired in the insulin resistant state, resulting in elevated circulating NEFA in combination with the anabolic hormone insulin, which promotes aberrant storage in non-adipose tissues [15]. Furthermore, the elevated TAG content of obese adipocytes provides increased substrate, resulting in increased NEFA generation [15]. The uptake of circulating NEFA by cells occurs via passive diffusion or through transporter proteins such as CD36 located in the cell membrane [15]. Fatty acyl-CoAs are either esterified, increasing TAG content, or directed to undergo β -oxidation [15]. Excessive TAG storage and hydrolysis can result in the build-up of metabolites such as fatty acyl-CoAs, diacylglycerols (DAG) and ceramides, leading to lipotoxicity, which has been studied in renal tubule cells [16].

Effects of ectopic TAG over storage on insulin signaling have also been studied, but this work has primarily been conducted in hepatocytes and myocytes, because of the important role of these cells in blood glucose regulation and disposal [15]. In hepatocytes, accumulation of these lipid metabolites causes continuous activation of serine/threonine kinases (i.e. protein kinase C (PKC)), which subsequently inhibits the phosphorylation of insulin – receptor substrates (IRS) and thereby decreases phosphatidyl-inositol-3-kinase (PI3K) activity [15]. In addition to IRS and PI3K, the action of transcription factors such as forkhead box O (FOXO), which activates enzymes involved in gluconeogenesis, is also impaired [15]. The collective downstream effect interferes with insulin signaling, subsequently resulting in decreased hepatic glucose uptake and increased glucose production, contributing to an overall increase in plasma

glucose levels [15]. In myocytes, impaired insulin signaling leads to decreased GLUT4 recruitment and therefore decreased glucose disposal post-prandially [15, 17].

TAG accumulation in organs such as the heart, skeletal muscle and the liver has been shown to impair major tissue functions, such as contractility, and also cause changes associated with metabolic syndrome, such as disturbances in local and systemic glucose metabolism [15]. Whether ectopic lipid accumulation in renal tubule cells causes alterations in kidney or systemic glucose metabolism, however, is poorly understood.

Previously, the Lipid Enzyme Discovery lab has investigated the male RTSAKO mouse model and found changes to glucose tolerance with no alterations to insulin sensitivity at 16-18 weeks of age. Clamping studies further demonstrated that they are not insulin resistant at the level of various organs, including adipose tissue, skeletal muscle, and liver, but rather that they have a deficiency in insulin secretion. Subsequently, lysophosphatidic acid (LPA), a bioactive phospholipid, in serum and kidneys of the male RTSAKO mice (unpublished data) was found to be elevated. Treatment with an LPA receptor inhibitor reversed the glucose intolerance and restored insulin secretion in the RTSAKO mice to control levels, demonstrating a causal role for LPA in impaired glycemic control. The current thesis focuses on aged female RTSAKO mice to determine if they develop a similar phenotype to that of the younger male RTSAKO mice, but with a longer latency.

The Role of Kidney in Blood Glucose Regulation

The involvement of the kidney in producing and utilizing glucose is understudied, since it is primarily considered to be a filtration system [18]. In general, the kidney functions to filter plasma, reabsorb essential substances and secrete waste in the form of urine [18]. Therefore, the renal system is crucial in regulating fluid and electrolyte balance, but it also plays important roles

in glucose homeostasis [18-21]. Utilization and release of glucose occur in the renal medulla and renal cortex, respectively [18]. The renal medulla has glycolytic and glucose phosphorylating enzymes, which enable accumulation of glycogen for its own use [18]. Conversely, the renal cortex mainly expresses gluconeogenic enzymes such as glucose-6-phosphatase, which enables the de novo synthesis and release of glucose into the circulation [18]. Therefore, due to the specificity of the enzymes present in the renal cortex and renal medulla, each area is predominately limited to activities involving either the utilization or production of glucose [18].

The kidneys aid in maintaining glucose homeostasis in three ways: endogenous renal glucose utilization, uptake and release of glucose via glucose transporters and de novo synthesis, and release of glucose into circulation via gluconeogenesis [19]. Following a meal, the kidney increases the uptake of glucose due to postprandial insulin stimulation [19]. As well, during the post-absorptive state, the kidney uses 10% of the body's total glucose reserve [19-21]. Therefore, the kidney, or more specifically the renal medulla, consumes glucose as a fuel source to ensure proper function [18].

In addition, it is approximated that 180 grams of glucose is filtered from plasma daily and reabsorbed from the urinary filtrate via glucose transporters (GLUTs) and sodium-coupled glucose cotransporters (SGLTs) present in renal tubule cells [18, 19, 21]. The GLUTs and SGLTs have a maximum capacity, and therefore exceeding the threshold, as occurs in both T1DM and T2DM patients, results in glucosuria [18]. The function and presence of each transporter varies in the kidney [18]. SGLT2 is particularly important, as it is responsible for reabsorbing 90% of the filtered glucose, whereas SGLT1 accounts for only 10% [18]. GLUTs are involved in passive diffusion of glucose, unlike the active transport by the SGLTs [18]. In the kidney, GLUT2 is the main transporter responsible for releasing glucose that was reabsorbed by

SGLTs at the apical side back into the circulation at the basolateral side of renal tubule cells [18]. Therefore, these transporters are key in mediating and regulating the uptake and release of glucose.

In humans, in the post-absorptive state, the liver is the primary source of free glucose, and the major source of blood glucose arising from de novo gluconeogenesis. However, recent studies have estimated the kidneys to contribute approximately 20% of total body glucose through gluconeogenesis in the post-absorptive state [18, 19]. Notably, the liver and kidney are the only organs known to contain physiologically relevant concentrations of the enzyme glucose-6-phosphatase that is essential for releasing glucose from glycogen, or newly synthesized glucose, to the circulation [19]. During the post-prandial state, however, there is a two-fold increase in renal gluconeogenesis, and the kidney becomes accountable for 60% of the endogenously released glucose [19]. On the contrary, hepatic gluconeogenesis is reduced by 80% and much of the incoming absorbed glucose is used to replenish hepatic glycogen stores, in a concept referred to as hepatorenal glucose reciprocity [19]. Although the kidney is not widely recognized as a source of free glucose like the liver, through its various activities, it plays an important role in the homeostasis and regulation of blood glucose [18-21].

Renal Lipid Accumulation

Studies have examined the pathways by which ectopic fat accumulation affects glucose and insulin regulatory cell signaling in the liver, skeletal muscle and heart. However, none exists in isolated in vivo kidney models [18]. Renal ectopic lipid accumulation (renal steatosis) has only recently been confirmed to occur in obesity [16]. While studies have investigated effects of renal steatosis on renal health and systemic glucose metabolism, models have not been targeted. For example, Deji et al. have studied renal health in mice fed a high fat diet (HFD) [22]. This

model of generalized obesity is associated with a host of systemic endocrine and metabolic alterations that confound the understanding of a kidney-specific role [22]. Kidney health has also been studied in mice globally deficient in the enzyme *Adipose Triglyceride Lipase* (ATGL) [23]. However, this whole-body knockout model causes ectopic fat storage in all organs, and alterations in systemic glucose handling [24]. Therefore, a targeted model of ectopic renal lipid accumulation would render insightful information on kidney health and blood glucose regulation exclusive of confounding factors.

Age Related Changes in Female Health

A “one-size-fits all” approach to adults is used in much of health care management, treatment and prevention [25]. Although such a notion is widely held, the need to address and distinguish sex-based differences has gained understanding in the past few decades [25]. Therefore, the role of aging in female health and disease is given greater attention in science and medicine [25]. Women have been shown to acquire disease differently than men, since they have an increased risk of strokes, CKD, various autoimmune diseases and osteoporosis, with age [25, 26]. The body composition and the overall shape of females is thought, in-part, to affect these observed differences [25]. In 1947, Vague described women as “pear-shaped” and therefore having more subcutaneous fat than visceral fat [27]. Fat distribution, which is measured by waist circumference relative to hip circumference, is a predictor of the risks associated with developing certain diseases such as cardiovascular disease [27].

In addition to the body fat distribution, another factor that affects women’s health and disease development is their age [27]. Significant increases in various diseases are observed amongst women after menopause, and the sex-based difference this causes is evident as women encounter their first myocardial infarction about 10 years later than men [27]. The post-

menopausal period, which is associated with a loss of ovarian hormones, brings about a redistribution of the body fat from subcutaneous to visceral locations [27]. In comparison to subcutaneous fat, higher adiposity in the visceral compartment is known to result in increased FFA delivery to the visceral organs [27]. Therefore, in combination with a loss of estrogen and a relocation of adipose tissue in females with age, their risk of developing ectopic lipid storage in visceral organs is significantly heightened [15, 27]. The best-known example of this, and the most studied, is nonalcoholic fatty liver disease (NAFLD) [27].

In experimental rodent models, ovariectomy has been shown to cause an accumulation of liver TAG content [27]. Similarly, treatment with 4-vinylcyclohexene diepoxide (VCD) to chemically deplete estrogen sources in mice has led to insulin resistance, dyslipidemia and fatty liver [27]. Alterations to female health as a result of age seems to predominately be associated with a decline in ovarian hormones, especially estrogen, however, long-term exposure to other signaling molecules that are not commonly considered, such as lysophosphatidic acid (LPA), may also contribute to the increased risk of atherosclerosis, cardiovascular disease and possibly changes to glucose metabolism [27, 28]. Notably, the study of a specific role for renal ectopic lipid accumulation in the health of aged females has not yet been reported, and is warranted, given parallels to the health of post-menopausal women.

An Appropriate Mouse Model

In order to investigate the effects of renal steatosis in isolation, the Lipid Enzyme Discovery Lab has generated a novel mouse model with a defect in the process of lipolysis. Studies have identified enzymes crucial for the process of lipolysis, one of which is identified as desnutrin/adipose triglyceride lipase, and it is involved in catalyzing the hydrolysis of TAG, forming DAG and a free fatty acid [29, 30]. The importance of ATGL is evident in ATGL-

deficient mice, and in patients with mutations in the *ATGL* gene, since both the mice and humans show reductions in lipolysis and therefore lipid accumulations in various tissues of the body [30]. Therefore, our lab has created mice that are deficient in *Atgl* in the renal tubules of the kidney, in order to impair fat breakdown, and increase TAG content.

Members of our laboratory have characterized young Renal-Tubule Specific *Atgl*-Knockout (RTSAKO) mice and have found that at age 16-18 weeks, male mice display glucose intolerance with no changes to insulin sensitivity (unpublished data). However, female mice at the same age show glucose metabolism that is comparable to their control littermates, and they are both glucose tolerant and insulin sensitive. Therefore, a sexual dimorphism exists, although both males and females at a young age show no evidence of renal lipotoxicity or changes in renal glucose handling. Mechanistic studies have been performed, and it has been determined that young male mice have elevated plasma LPA levels. LPA is a bioactive phospholipid mediator produced by adipocytes that acts via 6 different G-protein-coupled receptors (i.e. LPAR 1 – 6) [31, 32]. Work by other groups has demonstrated that LPA can impair glucose metabolism by decreasing plasma insulin secretion [31]. Researchers in our laboratory have found that an LPAR1/3 receptor antagonist can restore insulin secretion and glucose tolerance in the glucose intolerant male RTSAKO mice at age 16-18 weeks. Data from a collaboration between the Stark and Duncan labs has shown that female mice at 16-18 weeks of age, however, do not have significantly elevated lysophosphatidic acid levels, strongly suggesting that the lack of glucose dysregulation is due to the lack of differences in this bioactive lipid. A manuscript detailing this work is currently under preparation. However, questions remain regarding the phenotype of RTSAKO mice, and the role of elevated renal TAG content in kidney health and glycemic control, particularly in aged animals. In humans, diabetes rates are similar between men and

women, but there is a later onset in females [25, 33]. Whether female RTSAKO mice develop impaired glycemic control at a later age, and whether chronic exposure to ectopic TAG over-storage leads to eventual changes in kidney metabolism and health, has not yet been investigated.

Present Research Interests

To date, work completed by other members of our laboratory on 6-month old female RTSAKO mice indicate glucose tolerance comparable to their littermate controls. However, as mentioned previously, males develop glucose intolerance at the very early age of 16 – 18 weeks. Therefore, current interest lies in examining an older timepoint in females to investigate if metabolic changes comparable to males develop with age. Since human females have a latency in disease development, it is plausible to expect such trends in the RTSAKO mice, although a direct comparison cannot be made between the human and murine model [27, 34]. For the purposes of this project, 14-16-month-old RTSAKO mice have been chosen. We have used this specific timepoint since it is significantly later than previous timepoints used (i.e. 6 months of age) and mice after the age of 6 months are known to have a maturational rate that is 25 times faster than humans [34]. Thus, in comparison to human age, the 14-16-month-old timepoint is equivalent to approximately 47 – 53 human years [34]. Since human females begin to enter menopause at an average age of 51 years, the 47 – 53 age range provides flexibility in understanding age related changes to female health as a result of renal steatosis [34, 35]. In addition, mice are known to enter perimenopause by 9 month and begin transitioning into reproductive senescence around the 9-12-months of age [34, 36]. Therefore, this chosen timepoint overlaps between menopause and reproductive senescence in female humans and mice, respectively [27, 34-36].

The following research aims to investigate changes to health as a result of renal steatosis using aged female RTSAKO mice. Renal steatosis is investigated by measuring kidney weights, and renal lipotoxicity and inflammation by assessing the expression of biomarker genes of inflammation, fibrosis and proliferation. Glucose metabolism is examined through glucose and insulin tolerance testing, and physical activity and energy expenditure are measured using the comprehensive lab animal monitor system (CLAMS). The examination of these measures in aged females with potential renal steatosis are understudied in the current literature [37]. Thus, my research will fill knowledge gap regarding the effects of kidney health and glucose metabolism, while also investigating if the 14-16-month-old female RTSAKO mice recapitulate the phenotype of the younger male RTSAKO mice.

Chapter 2: Biochemical Foundations

Introduction

Understanding the effects of renal steatosis in RTSAKO mice on kidney health and whole-body glucose metabolism requires background knowledge on renal lipolysis. Therefore, the following section will first provide an overview of lipolysis. It will also examine the contribution and function of key enzymes, signaling molecules and various hormones involved in this process with attention to potential roles in the pathology of renal lipid accumulation and the development of metabolic diseases such as diabetes mellitus.

Lipolysis

During the fasting state in which the body must derive energy from stored sources, triacylglycerols (TAG), which are chemically inert molecules stored in the cytosol of cells as lipid droplets are hydrolyzed into non-esterified fatty acids (NEFAs) [30, 38]. NEFAs released through lipolysis from adipocytes can travel through the circulation and enter peripheral tissues to undergo β -oxidation to generate necessary amounts of ATP [30]. Virtually all cells of the body are able to store and mobilize TAG. However, non-adipose tissues such as kidney do not release liberated NEFA, but rather use them endogenously for energy production [30].

The hydrolysis of TAG is regulated by specific enzymes referred to as lipases. There are currently three major lipases that have been identified as functioning in the process of breaking down TAG into NEFA plus a single molecule of glycerol [30, 38]. Adipose triglyceride lipase is involved in catalyzing the first step which is rate-limiting [30]. Here, TAG is hydrolyzed into diacylglycerol and NEFA [30]. The second step uses hormone-sensitive lipase (HSL), which is a multifunctional enzyme, since it is able to hydrolyze DAG into monoacylglycerol (MAG) and

NEFA, but also TAG into DAG and NEFA [30]. Finally, monoglyceride lipase (MGL) is involved in cleaving MAG into glycerol and NEFAs [30].

The concentration of NEFA is tightly regulated in the cell by TAG hydrolysis and NEFA esterification. The balance between these two processes is critical to the cell, since any deviations may result in lipid accumulation and therefore lipotoxicity [30, 39].

Adipose Triglyceride Lipase

Adipose Triglyceride Lipase, known for its hydrolysis of TAG into DAG and NEFAs, was first identified in 2004 by three different groups, and therefore has also been referred to as desnutrin and patatin-like phospholipase domain containing protein 2 (*Pnpla2*) [30, 40, 41]. Previously unknown, the stereoselectivity of ATGL was thought to be primarily at the *sn*-1 rather than the *sn*-2 position of TAG [30, 42]. Hydrolysis of TAG by a lipase can result in one of three different isoforms of DAG: *sn*-1,3, *sn*-1,2 and *sn*-2,3 DAG [42]. A recent study has shown ATGL to preferentially generate *sn*-1,3 DAG, and undetectable amounts of *sn*-1,2 DAG indicative of TAG hydrolysis at the *sn*-2 position rather than the *sn*-1 [42]. However, TAG hydrolysis in the presence of the ATGL co-activator CGI-58 provides a greater variation of products, as it yields both *sn*-1,3 and *sn*-2,3 DAG [42].

The murine *Atgl* gene encodes for a 486-residue protein and generates an mRNA that is approximately 2.6 kb long. When comparing the human and murine ATGL, they share about 84% similarity in amino acid identity. *Atgl* mRNA is expressed in various types of tissues with the highest expression in white adipose tissue (WAT), brown adipose tissue (BAT), liver and kidney and a lower expression in the testis, skeletal and cardiac muscle [43].

The importance of ATGL activity is evident in studies examining experimental models with ATGL deficiencies [44]. The hydrolysis of TAG by ATGL is mediated by the catalytic

serine-aspartate dyad (Ser47-Asp215) and their presence is critical for the activity of the enzyme [30]. In a mutation study in which Ser47 was replaced with an alanine, this resulted in an inactive protein, therefore causing TAG accumulation [30]. This further indicates that having a functional ATGL enzyme is essential in preventing TAG accumulation, and is indispensable in the physiological function of adipose and non-adipose tissue [30].

Hormone-Sensitive Lipase

The role of hormone sensitive lipase as an enzyme involved in catalyzing the second step of TAG hydrolysis was first discovered in WAT [30]. Activity of this enzyme is prominent during times of fasting, and its intracellular activity is stimulated by catabolic hormones such as glucagon and catecholamines [45]. Although HSL is capable of hydrolyzing various substrates from MAG, DAG, TAG, cholesterylesters and retinylesters, the ratio of the relative rates for each are 1:10:1:4:2, respectively [30]. Therefore, HSL demonstrates a greater preference for the hydrolysis of DAG than any other substrate [30].

Otherwise referred to as LIPE, the murine *Hsl* gene is approximately 10 kb long and encodes for a 2.8 kb mRNA transcript [45]. The expression of HSL is tissue-specific, where it is highly expressed in WAT and BAT, and there are lower rates of expression in muscle, steroidogenic tissue, and pancreatic β -cells [30]. The structure of HSL is thought to encompass three regions: the N-terminal, C-terminal and a regulatory area [30]. The N-terminal is involved in lipid binding and interactions with proteins such as fatty acid binding protein [30]. The C-terminal consist of α/β hydrolase folds, which contain the catalytic triad which is Ser424-Asp693-His723 in the murine protein [30, 46]. The final regulatory region of HSL contains the five phosphorylation sites [30].

During the process of lipolysis, catabolic hormones activate adenylate cyclase, which results in increased amounts of cyclic adenosine monophosphate (cAMP) [47], therefore causing protein kinase A (PKA) to become active as its catalytic and regulatory subunits dissociate from each other in response to cAMP binding [47]. The phosphorylation of HSL by PKA has been shown to promote the interaction between HSL and the lipid droplet, thereby promoting the hydrolysis of subsequent lipid molecules [47]. In rodents, HSL is known to be phosphorylated by PKA at three sites: Ser563, Ser659, and Ser660 [47]. Although studies continue to investigate additional phosphorylation sites in HSL, it is currently acknowledged that phosphorylating HSL allows it to gain a flexible conformation needed for translocation and a rapid turnover rate [47].

Monoglyceride Lipase

Monoglyceride lipase is an enzyme first discovered in rodent adipose tissue for its function in hydrolyzing MAG. It is encoded by a 4.6kb mRNA transcript, coding for a 303-residue protein [30, 48]. The level of *MGL* mRNA expression is notably high in the kidney, testis and adipose tissue [30, 48]. It catalyzes the last step of TAG hydrolysis, and unlike other lipases, it is not multifunctional and therefore does not display any activity towards TAG or DAG [30]. Thus, the function of monoglyceride lipase is limited to MAG hydrolysis alone.

Lysophosphatidic Acid

Lysophosphatidic acid is a water-soluble bioactive phospholipid present in a number of different tissues, and it acts via G protein-coupled receptors (GPCRs) [31, 32]. Its signaling affects various cellular processes such as proliferation, differentiation, and the survival of cells [49]. LPA acts as an intra- and extracellular signaling molecule, and can be synthesized through four different pathways: 1) cleavage of lysophospholipids (LPL) such as lysophosphatidylcholine (LPC) by lysophospholipase or autotaxin; 2) the hydrolysis of phosphatidic acid (PA) by

phospholipase A₁ and A₂; 3) phosphorylation of MAG by monoacylglycerol kinase; and 4) acylation of glycerol 3-phosphate using glycerophosphate acyltransferase [31, 32]. LPA generated in cell signaling is primarily produced from the first two pathways, while the latter pathways produce LPA for use in the cellular de novo synthesis of glycerolipids [31].

To date, six different LPA receptors (LPAR) have been identified through which biological activity of LPA is mediated. These receptors have seven helices that span across the cellular membrane, and are coupled to different GPCR, including G α_i , G α_s , and G α_o , which can thus exert very different net outcomes, depending on relative expression in a particular cell [32]. Levels of LPAR expression are cell specific, and can even vary across similar tissues, such as various adipose depots [50]. Thus, the cellular profile of LPAR influences the outcome of LPA-mediated signaling on cell function [32].

LPA, previously viewed as an inert metabolite, gained a greater recognition as its implication in various human diseases became evident [32]. The role of LPA in diseases such as cancer [51], cardiovascular disease [52], reproductive disorders [49] and neuropathic pain [53] has been investigated using various experimental models [31]. A study examining unilateral ureteral obstruction as a model of renal fibrosis in mice found an elevation of LPAR1 [31]. Fibrosis is a condition characterized by the buildup of excess fibrous connective tissue, and its presence affects the functional and structural integrity of the cells and organs of the body [31]. Studies have shown LPA to strongly influence fibrosis through its various LPARs by increasing the expression of growth factors such as connective tissue growth factor in renal fibroblast cells [31, 54]. As well, reduction of renal fibrosis was shown in *Lpar* knockout mouse models, and when LPA inhibitors such as Ki16425 were used [31, 54]. Our laboratory has previously found increased LPA in the kidney and blood of young male RTSAKO mice. Although LPA was not

elevated in the blood of young female mice, it is possible that production of this molecule may increase in the kidneys and blood of female RTSAKO mice after prolonged steatosis exposure, and this may increase the risk for fibrosis. Studies on the health of RTSAKO kidneys, including any changes in fibrosis, are therefore warranted in aged female mice.

Studies on a role for LPA in regulating glycemic control of aged female RTSAKO mice are also warranted, based both on findings from our laboratory, and on prior work from the literature [55-57]. A role for LPA in insulin secretion and blood glucose regulation has previously been established, and a specific role for LPA in the regulation of these processes in the young male RTSAKO mice has been discovered by our laboratory [55, 56]. The 16-18-week-old male RTSAKO mice have elevated levels of LPA, and they are glucose intolerant, insulin sensitive and have a low concentrations of insulin, while the 6-month old female RTSAKO mice do not exhibit such changes. As well, acute treatment with Ki16425 to the male mice has been shown to rescue the intolerance (unpublished data). Since insulin sensitivity remains unaltered and glucose tolerance is affected in the male RTSAKO mice, elevated levels of LPA are thought to impact insulin secretion. Studies by Rancoule et al., have examined this effect, and found that LPA impairs glucose homeostasis in HFD-fed mice by inhibiting insulin secretion [55]. In that study, mice fed a HFD developed increased circulating LPA levels. When exogenous LPA was given mice fed either a normal diet or a HFD, glucose tolerance was impaired in both groups, but more so in the HDF mice [55]. Interesting, plasma insulin levels were also decreased as a result of LPA injection [55]. However, treatment with Ki16425 prior to administering exogenous LPA not only rescued the glucose intolerance, but also levels of plasma insulin, indicating that such deleterious outcomes can be negated by blocking LPA receptors and, thus, the signaling action of LPA [55]. Moreover, chronic treatment of Ki16425 in HFD-fed mice was found to modestly

increase the number of islet cells, without changing the size or number of cells per islet [55]. Although inconclusive, an increase in the number of islets is associated with an increase in the number of beta cells since these cells comprise 95% of the islets [55]. Since chronic treatment with Ki16425 had only a minor effects on one aspects of the beta cells (i.e. size), it is unclear if the effect is direct or indirect. However, in acute studies with a single injection of Ki16425, a rescue of insulin levels was achieved, indicating that long-term effects on islet cell numbers could not explain that effect. Studies to understand the mechanism underlying the link between LPA and impaired insulin secretion are the topic of confidential work in our lab and will not be discussed here.

Insulin

Insulin is a dipeptide hormone containing A and B chains, and it is synthesized by the β cells of the pancreas [58, 59]. It is secreted in response to hyperglycemic conditions, and functions to maintain physiological blood glucose levels via cellular glucose uptake [59]. The release of insulin in response to increased levels of glucose is biphasic [59]. In the first phase, a pulse of insulin is rapidly released, typically occurring in the first minute or two after glucose exposure [59]. The second phase is slower in response and begins at least 10 minutes after the ingestion of glucose, typically occurring within 10 to 20 minutes [59]. In comparison to the first, the second phase lasts the duration of the hyperglycemia and represent insulin that is both stored and newly synthesized in proportion to the glucose ingested [59]. Insulin acts via an insulin receptor that contains 2α and 2β glycoprotein subunits connected by a disulphide bond [58, 59]. Binding of insulin to the receptor causes phosphorylation of the insulin receptor substrate (IRS) which then mediates downstream signaling and modulates the various cellular actions of insulin [59].

Insulin resistance is a common occurrence amongst various diseases, especially in T2DM [59, 60]. In these individuals, plasma insulin concentrations are normal or even higher, however, due to post-receptor defects at the cellular level, insulin signaling is impaired, which is termed insulin resistance (IR) [59]. When the β cells are unable to compensate for the IR, glucose intolerance follows [59]. Therefore, proper release of insulin and its function of its receptor substrates are crucial for preventing known metabolic diseases [59, 60].

Glucagon

Glucagon is a 29 amino acid-long peptide hormone secreted by the α cells of the pancreas [61, 62]. Initially discovered in the 1920's as an impurity, the hormone has various functions, however, it is primarily involved in increasing blood glucose via glycogenolysis and gluconeogenesis [61, 62]. Glucagon is derived from a proglucagon precursor and acts via a G protein-coupled receptor, which is commonly found in the liver, kidney, heart and adipose tissue [62]. The release of glucagon is in response to hypoglycemic condition sensed by the hypothalamus and parasympathetic nervous system [62]. In addition to glucose metabolism, glucagon affects lipid, protein as well as energy metabolism and therefore acts to maintain a constant supply of fuel to all organs [62].

T2DM patients have impaired glucagon regulation during the fed and fasted states [61]. During the fed state, when glucagon levels are ideally low, T2DM patients exhibit a higher concentration, which may indicate resistance to insulin at the level of the α cells [61]. However, the exact mechanisms causing hyperglucagonemia are not fully understood [61].

Leptin

Leptin is a hormone secreted by white adipose tissue, and is a 167 amino acid-long product encoded by the leptin gene [63, 64]. First discovered in *ob/ob* mice, it is secreted in a pulsatile fashion and fluctuates in concentration throughout the day, as high levels are observed in the evening and morning hours [63]. Leptin is involved in the regulation of energy homeostasis, neuroendocrine and metabolic functions [63]. It acts through specific leptin receptors that are localized in the brain and various peripheral tissue [63]. Increases in leptin cause a reduction in appetite, increased energy expenditure, and lead to weight loss [63, 64]. In obese individuals, leptin resistance is a very common occurrence, although the mechanism by which it happens is partly unknown [63, 65]. However, individuals with a homozygous leptin gene mutation are known to be morbidly obese very early in life [63]. As a result, improper leptin function plays an important role in promoting obesity [63]. In addition, leptin has also shown to regulate glucose homeostasis [63, 66]. When exogenous leptin is administered to *ob/ob* mice, blood glucose is lowered [66]. Therefore, it is suggestive that deficits in leptin signaling may lead to alterations in glucose metabolism [66].

Resistin

Resistin is a 108 amino acid-long peptide belonging to the resistin-like molecule hormone family, and secreted by adipocytes and macrophages in mice and human, respectively [67, 68]. It is named for its ability to counter or resist the actions of insulin and suppress insulin mediated glucose uptake in cells [68]. However, there is an ongoing debate about its exact role in obesity, insulin resistance and the development of T2DM [68]. Resistin is also known to be implicated in the development of NAFLD, CVD, atherosclerosis and CKD [68]. Studies in 2001 revealed an increase in plasma resistin levels in diet-induced obese mouse models [67, 68]. Subsequent

treatment with an anti-resistin antibody was shown to increase insulin sensitivity in these mice [67]. As well, healthy mice given recombinant resistin caused impairments to insulin action and glucose intolerance [67]. Since the majority of the work regarding resistin was completed in murine models, the applicability of the findings was questioned, as resistin production is dependent on the species [68]. However, despite the controversy, resistin is still considered to play an important role in various metabolic diseases [67, 68].

Chapter 3: Phenotypic Characterization and Renal Expression of Select Genes Involved in Lipolysis, Lipogenesis, Inflammation, Fibrosis, and Proliferation in the 14-16-Month-Old Female RTSAKO Mice

Rationale: RTSAKO mice have been engineered with an intentional change in lipid metabolism in the proximal and distal renal tubules. ATGL, the enzyme responsible for catalyzing the first step of TAG hydrolysis, is non-functional in the RTSAKO mice, and therefore an accumulation of TAG is expected to result in renal tubule cells (i.e. ectopic lipid accumulation, or renal steatosis) [23, 44]. Renal steatosis is known to occur in metabolic diseases such as obesity and diabetes [69, 70]. However, in RTSAKO mice, renal steatosis develops independently of obesity or other metabolic diseases. This allows for the study of the role of renal steatosis in the development of metabolic disease, rather than the study of renal steatosis as an outcome of systemic metabolic changes. Such a model is necessary to avoid confounding caused by systemic endocrine and metabolic alterations that are commonly present in models of generalized obesity [22]. As a result, this model allows for inference of a *causal role* for renal steatosis in metabolic disease, which is a significant strength.

Aging causes physiological, functional and degenerative changes to the organ systems, and therefore individuals at older time points may present a different phenotype than individuals studied as young adults [71]. Studying RTSAKO mice at older ages will provide important information on the effects of chronic renal steatosis on kidney and whole-body health outcomes. Thus far, our laboratory has performed phenotypic characterization of young male and female RTSAKO mice at ages 9-18 weeks. This work demonstrated the presence of compromised glycemic control in 16-18-week-old male, but not female, RTSAKO mice. Additional preliminary studies on glycemic control in 4-month and 6-month old female mice has shown, similarly, that impaired glycemic control does not yet develop. In humans, pre-menopausal

women have lower rates of chronic disease than men, although these rates rise to equivalency after menopause [27]. Although mice do not undergo menopause, they do experience a reproductive decline and senescence [34, 36]. Therefore, studying female RTSAGO mice at the age of 14-16 months, which corresponds to this period, may provide insight into the specific effects of renal steatosis on health in aging.

In any new animal model, it is important to establish a basic phenotype, including specificity of the genetic model. In the RTSAGO model, *Atgl* gene excision is driven by Cre recombinase that is under control of the kidney-specific cadherin (Ksp) promoter [72, 73]. This promoter has been well characterized in young mice as highly specific to the renal tubules of the kidney, but it is important to determine that in aged mice, it is not aberrantly induced in other tissues as well, since this could affect interpretation of studies on metabolism, and even invalidate the use of this model.

It is also important to establish a basic characterization of organ and tissue weights prior to performing studies on metabolic control, since adipose tissue and liver are important regulators of glycemia. Thus, changes in adiposity, or evidence of hepatosteatosis, both of which would be evidenced by changes in tissue mass, could confound the interpretation of a kidney-specific role in any observed effects, and are therefore important to determine in initial studies.

Finally, it is important to establish the basic phenotype and health of the kidneys, as the target organ in this model. Long-term exposure of renal tubules to elevated TAG overstorage could lead to lipotoxicity [16, 39]. This could potentially cause inflammation, fibrosis, and the activation of proliferative mechanisms in the kidneys, which could also lead to metabolically significant extra-renal effects, such as IR resulting from the release of inflammatory cytokines by the damaged organ [16, 39]. Thus, the expression of select genes involved in inflammation (*i.e.*

Tnfa, *Il-1 β* , *Il-6*), fibrosis (*i.e.* *Colla1*, *Col4a1*, *Fn-1*) and repair (*i.e.* *Pcna*, *Ki67*) were assessed. Notably, these processes are controlled primarily through transcriptional regulation, and therefore gene expression analysis provides a useful surrogate measure reflecting the extent of activation of these processes [74]. Furthermore, long-term exposure of renal tubules to elevated TAG over storage could also induce compensatory effects on lipid metabolic pathways, including upregulation of *Hsl*, the other major cellular lipase with TAG hydrolase activity, and downregulation of the expression of enzymes implicated in lipogenesis (*i.e.* *Dgat1*, *Lipin1*). *Lipin1* is a phosphatidic acid phosphohydrolase that dephosphorylates phosphatidic acid to make DAG [75], while *Dgat1* catalyzes the final step of TAG biosynthesis from DAG, and therefore these enzymes are directly implicated in the regulation of cellular TAG production [76]. Notably, however, although enzymes in lipolysis and lipogenesis are regulated transcriptionally, at least in part, the activity of these proteins is also significantly modulated post-translationally by modifications such as phosphorylation [74, 77]. Future work should include direct determination of levels of the proteins, including measures of important modified forms.

Objectives:

1. To confirm renal expression of Cre-recombinase
2. To examine body weights, gross tissue masses, and renal gene expression of lipid metabolism enzymes and inflammation, proliferation, and fibrosis markers in RTSAKO mice and control littermates at 14 – 16 months of age.

Hypotheses:

1. The expression of Cre-recombinase will be exclusive to the kidneys of the RTSAKO mice.

2. Body weights will be similar between RTSAKO and control littermates, since kidneys account for only 2-5% of body mass.
3. Kidney weights will be higher in the female RTSAKO mice compared to control littermates due to an overstorage of TAG, but other organs are not expected to differ in mass.
4. Expression of genes involved in lipid synthesis will be decreased, and expression of *Hsl*, a gene involved in lipid breakdown, will be increased. Gene expression of cytokines, proliferation markers, and enzymes involved in fibrosis will be elevated.

Methods:

Study Design

All protocols were approved by the Animal Care Committee at the University of Waterloo (AUPP# 30053). The mice were bred and housed at the Central Animal Facility at the University of Waterloo in group housing with a chow diet and water. The conditions in which they are housed are controlled to a 12h hour dark and light cycle with constant temperature. Female RTSAKO and control mice age 14-16 months were used for this study.

RTSAKO Knockout Mouse Model

To create RTSAKO mice, the *Cre-LoxP* recombination system was used to excise the catalytic region of *Atgl* in the epithelial cells of the renal-tubules. Mice homozygous for floxed *Atgl* were a kind gift from Dr. Hei Sook Sul at the University of California, Berkley [78]. These mice have the first exon of their *Atgl* gene flanked by *Lox-P* sites. They were bred with commercially available transgenic mice expressing *Cre*-recombinase controlled by a kidney-specific promotor (B6.Cg-Tg(Cdh16-cre)91Igr/J from Jackson Laboratories). Both *Atgl flox/flox* and transgenic mice were backcrossed >12 generations onto C57Bl/6J background prior to mating. *Cre*-recombinase is derived from a P1 bacteriophage and is able to excise genetic sequences between two *Lox-P* sites, resulting in either a deletion, inversion or translocation of the respective sequence [72]. In the RTSAKO mouse model, the expression of *Cre*-recombinase causes a deletion of the sequence coding for ATGL in the epithelial cells of the renal-tubules [78]. However, in the absence of expressed *Cre*-recombinase, *Atgl* remains flanked by the two *Lox-P* sites that do not interrupt the gene, and control littermates are produced [72].

To generate a mouse colony containing litters that are all homozygous for floxed *Atgl* with (knockouts) or without (controls) *Cre*-recombinase first requires matting *Atgl* flox/flox mice with *Ksp-Cre* transgenic mice [78]. This produces mice that are all heterozygous for floxed *Atgl*, with ~50% that are also heterozygous for *Ksp-Cre* (fig.1a), where the remaining 50% are control for *Cre* [78]. Subsequent mating of heterozygous *Ksp-Cre*/heterozygous *Atgl* floxed mice with mice that are homozygous for the *Atgl* flox/flox allele (fig.1b) results in progeny where 25% are homozygous for the *Atgl* floxed allele and transgenic for *Cre* [78]. To produce functional litters for experiments, *Ksp-Cre* transgenic mice homozygous for the *Atgl* floxed allele are crossed with *Atgl* flox/flox mice resulting in 50% of the mice expressing *Ksp-Cre* (knockouts) and 50% without *Ksp-Cre* (controls) (fig.1c) [78].

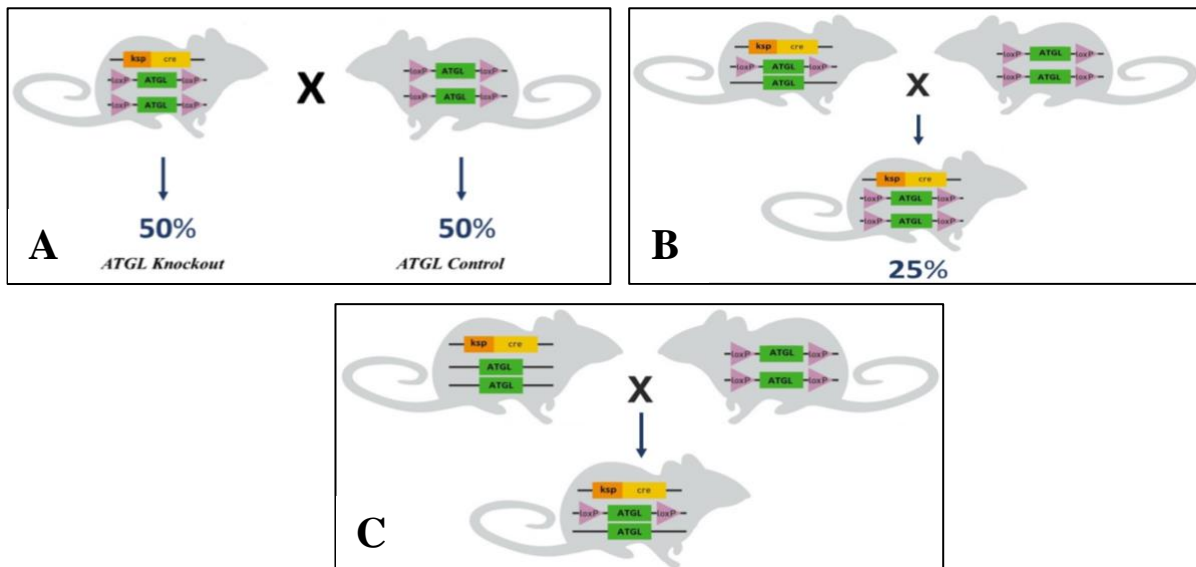


Figure 1: Breeding strategy for the RTSAKO and Control Mice

(A) The *ATGL* floxed mice are mated with the mice expressing *Ksp-Cre* transgenic mice to produce a progeny that is 50% heterozygous for *Ksp-Cre* and 50% control for *Cre*. (B) Mating of heterozygous *Ksp-Cre* mice with *Atgl* flox/flox mice yields progeny where ~25% are homozygous for the *Atgl* floxed allele and transgenic for *Cre*. (C) *Ksp-Cre* transgenic mice homozygous for the *Atgl* floxed allele are crossed with *Atgl* flox/flox mice resulting in progeny where 50% of the mice express *Ksp-Cre* and 50% do not express *Ksp-Cre*, creating the knockout and control littermate mice, respectively. Adapted from [79].

DNA Isolation

Mice were ear notched for DNA extraction and ear punches were placed in sterile 1.5mL microfuge tubes. The ear punches were digested in 100 μ L basic digestion buffer (25mM NaOH/0.2mM disodium EDTA) and heated at 95°C for 1 hour using the T100 Thermal Cycler [80]. Following cooling at 4°C 100 μ L of neutralization buffer (40mM Tris-HCl) was added and stored at -20°C for later use [80].

Genotyping

In order to genotype for *Cre* 1 μ L of DNA extracted for each mouse is pipetted into a sterile PCR tube along with 19 μ L of a reaction mixture containing 2 μ L of 10X PCR reagent with MgCl₂, 0.4 μ L of dNTP's Mix, 15.86 μ L of ddH₂O, 0.32 μ L of 20 μ M *Cre* forward and reverse primer and 0.1 μ L of 5U/ μ L FastStart Taq polymerase. The reaction mixture is placed in the T100 thermocycler under the following conditions: 95°C for 4 min, followed by 40 cycles of at 95°C for 30s (denaturation), 60°C for 30s (annealing), 72°C for 1 min (extension), and 72°C for 7 min. After the reaction is completed, approximately 3.33 μ L of loading dye is added per sample [73]. While the PCR reaction is occurring, a 1.5% agarose ethidium bromide (EtBr) gel is assembled by using Tris-acetate-EDTA (TAE) buffer to dissolve the agarose. An EtBr concentration of 5 μ L/100mL can be added to the solution once cooled. Once the gel solidifies in the casting tray, 5 μ L of 100bp DNA ladder is loaded in to the first well followed by the remaining samples with loading dye. The gel was run at 100V for 45mins – 1 hour in 1X TAE Buffer and imaged using the ChemiDoc™ Touch Imaging System under the EtBr setting using UV light. Once imaged, knockout mice or mice expressing *Cre*-recombinase are identified by the

270 bp amplicon that is produced as a result of the amplification [73]. However, control mice which do not express *Cre*-recombinase will not display any amplification.

RNA Extraction

To prevent degradation of RNA, the work environment was cleaned and sanitized using RNase ZAP. For RNA extraction, approximately a 100 mg was cut and placed in a 5mL falcon tube along with 1mL of chilled TRIzol reagent [50, 81]. Tissues were homogenized using a Polytron at maximal speed and incubated on ice for 5 minutes. To the homogenized tissue, 200 μ L of chloroform was added and inverted to mix evenly, followed by 2-3 minutes of incubation on ice [50, 81]. The samples were subsequently centrifuged at 4°C for 15 mins at 1200 rcf, where the resulting supernatant (RNA) was carefully transferred into a clean 1.5mL microfuge tube. To the supernatant 500 μ L of isopropanol was added, inverted and incubated on ice for 10 minutes. Next, the sample was centrifuged at 4°C for 10 minutes at 1200 rcf, and the resulting aqueous layer was discarded, and the pellet was resuspended in 1mL of 75% ethanol and vortexed briefly. The samples were centrifuged for the final time at 4°C for 5 mins at 7500 rcf, where the supernatant was discarded and the resulting pellet air dried for 5-10 minutes and resuspended in 50 μ L of Mili-Q water. To facilitate resuspension of the pellet heat blocked at 60°C for 15 mins. To determine the purity ($260/280 = 1.8 - 2.0$) and concentration of the isolated RNA samples, the Nanodrop-2000 spectrophotometer was used where 1 μ L of sample and 1 μ L of ddH₂O was used as the control [50, 81].

Real-Time Polymerase Chain Reaction (RT-PCR) and CDNA synthesis

To obtain 2 μ g of RNA for all samples, using the concentration of the isolated RNA appropriate sums of the sample and ddH₂O was added into a clean PCR tube to achieve a total

volume of 10 μ L. For CDNA synthesis, a reaction mixture containing 10X RT Buffer (2.0 μ L), 25 X dNTPs (0.8 μ L), 10X RT Random Primers (2.0 μ L), Reverse Transcriptase Enzymes (1.0 μ L), ddH₂O (4.2 μ L) was added to 10 μ L of the 2 μ g of RNA to achieve a total volume of 20 μ L [50, 81]. The samples were placed in the thermocycler for the following conditions: 25°C for 10 mins, 37°C for 120 mins, 85°C for 5 mins and 4°C at infinity [50, 81]. A 1/5 working solution was subsequently prepared using the stock solution for gene analysis and stored at -20°C.

Quantitative PCR (qPCR)

To analyse a gene of interest and its level of expression, the Bio-Rad CFX96 Touch Real-Time PCR Detection System was used. Using a 96 well qPCR plate, a reaction mixture containing the following was added: 5 μ L of SYBR Green master mix, 0.5 μ L of Forward and Reverse primer (gene of interest/housekeeping gene), 3 μ L of ddH₂O and 1 μ L of CDNA. The cycling condition for the samples were: 95°C for 2 minutes, 95°C for 10 seconds (40 cycles) and 60°C for 20 seconds [50, 81]. For gene analysis using SYBR Green a house keeping gene is needed, therefore for each sample, both the expression of the housing keeping gene and gene of interest was analysed. To quantify the expression of a particular gene, the following equation was used: $\Delta C_t = (C_{t(\text{gene of interest})} - C_{t(\text{housekeeping gene})})$, where C_t represents the number of cycles taken to achieve luminescence and break a predetermined threshold value [50, 81]. The relative gene expression of the knockout to the controls are compared using the equation $\Delta\Delta C_t = \frac{2^{\Delta C_t \text{ knockout}}}{2^{\Delta C_t \text{ control}}}$ and the fold differences between the knockouts and the controls are expressed as $\text{Fold} = 2^{-\Delta\Delta C_t}$. For the following, the expression of the gene of interest was normalized to the ribosomal 18S (housekeeping gene) since it is abundantly expressed in cells [82].

Table 1: Primers for Housekeeping Genes

Gene	Direction	Sequence	Amplicon Size
<i>18S</i>	<i>Forward</i>	5'-GATCCATTGGAGGGCAAGTCT-3'	113 bp
	<i>Reverse</i>	5'-AACTGCAGCAACTTTAATATACGCTATT-3'	

Table 2: Primers for Genes Implicated in Inflammation

Gene	Direction	Sequence	Amplicon Size
<i>TNFα</i>	<i>Forward</i>	5'-CAACGCCCTCCTGGCCAACG-3'	114 bp
	<i>Reverse</i>	5'-TCGGGGCAGCCTTGTCCTT-3'	
<i>IL1-β</i>	<i>Forward</i>	5'-CCTGCTGGTGTGTGACGTTCCC-3'	84 bp
	<i>Reverse</i>	5'-GGGTCCGACAGCACGAGGCT-3'	
<i>IL-6</i>	<i>Forward</i>	5'-GCTGGAGTCACAGAAGGAGTGGCT-3'	117 bp
	<i>Reverse</i>	5'-GGCATAACGCACTAGGTTTGCCGAG-3'	

Table 3: Primers for Genes Implicated in Fibrosis

Gene	Direction	Sequence	Amplicon Size
<i>FNI</i>	<i>Forward</i>	5'-ACATGGCTTTAGGCGGACAA-3'	114 bp
	<i>Reverse</i>	5'-TTCGGCAGGTATGGTCTTGG-3'	
<i>Col1A1</i>	<i>Forward</i>	5' – GAAACCCGAGGTATGCTTGA – 3'	84 bp
	<i>Reverse</i>	5'-TACATCCTCAGCTCCCTGGG-3'	
<i>Col4A1</i>	<i>Forward</i>	5' – CTGGAGAAAAGGGCCAGAT – 3'	117 bp
	<i>Reverse</i>	5'-ACCTGTCCGTGTTCAATTCCT-3'	

Table 4: Primers for Genes Implicated in Lipogenesis

Gene	Direction	Sequence	Amplicon Size
<i>Dgat1</i>	Forward	5'-CTGGATTGTGGGCCGATTCT-3'	94 bp
	Reverse	5'-ATACATGAGCACAGCCACCG-3'	
<i>Lipin1</i>	Forward	5'-CCTTAGGGAGCCGGAAGACT-3'	91 bp
	Reverse	5'-ATTGTTGGCGACTGGTCACT-3'	

Table 5: Primers for Genes Implicated in Lipolysis

Gene	Direction	Sequence	Amplicon Size
<i>Hsl</i>	Forward	5'-GGAGTCTATGCGCAGGAGTG-3'	80 bp
	Reverse	5'-ATACATGAGCACAGCCACCG-3'	

Table 6: Primers for Genes Implicated in Proliferation

Gene	Direction	Sequence	Amplicon Size
<i>KI67</i>	Forward	5' - AATCCAACCTCAAGTAAAC-GGG-G - 3'	127 bp
	Reverse	5' - TTGGCTTGCTTCCATCCTCA - 3'	
<i>PCNA</i>	Forward	5' - TACAGCTTACTCTGCGCTCC - 3'	88 bp
	Reverse	5' - TTGGACATGCTGGTGAGGTT - 3'	

Mice Used

Cohort 1	
Control	RTSAKO
67 2-2	64 2-1
67 2-3	64 2-2
68 2-2	64 2-3
69 2-1	64 2-4
69 2-2	65 2-1
69 2-5	65 2-3
70 2-1	66 2-1
72 2-1	66 2-3
72 2-3	67 2-1
72 2-4	
73 2-1	

CT n=11
RTSAKO n=9

Age at the time of experiment:
14 months

Statistical Analysis

Statistical significance between groups of mice will be assessed using the Student's t test.

Results are expressed as the mean +/- standard error of the mean (S.E.M). A P-value of <0.05 was accepted as statistically significant.

Results:

Expression of Cre-Recombinase: The expression of Cre-recombinase in the 14-16-month-old female RTSAKO mice was obtained by processing cDNA from the kidney, liver, pancreas, brain, skeletal muscle and heart with primers specific for Cre-recombinase. Genomic DNA was used as a positive control, and therefore a band is expected in lanes A and G of this blot at 270bp. As depicted in fig.2, Cre is exclusively expressed in the kidney, with a distinct, solid band appearing in lane A at 270 bp, and no other bands present in any other lanes except for lane G, which contains an amplicon derived from genomic DNA, verifying the kidney-specific nature of this model. Additional bands present below the 100bp mark are non-specific primer dimers.

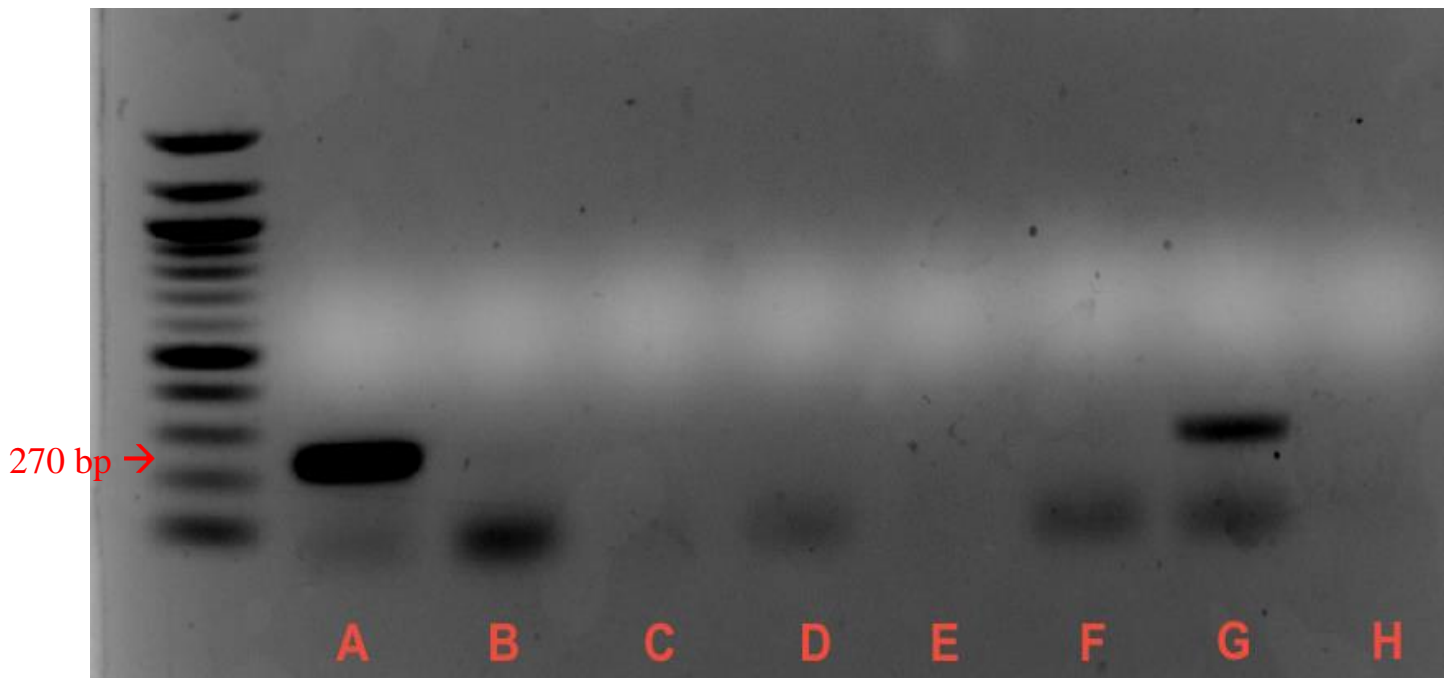


Figure 2: Expression of Cre-Recombinase

The expression of Cre-Recombinase tested in eight tissues of a single female RTSAKO mouse aged 14-16 months. These samples were run in a 1% agarose-TAE gel with a 100 base pair ladder. The samples analyzed in lanes A – F and H were prepared by tissue RNA extraction followed by reverse transcription and amplification by PCR using primers specific for Cre recombinase. Lane G is a positive control and shows an amplification of genomic DNA from the tail. (A) Kidney (B) Liver (C) Pancreas (D) Brain (E) Skeletal Muscle (F) Heart (G) Tail – as genomic DNA (H) Gonadal Fat.

Body and Organs Weights: As illustrated in fig. 3a, 14-16-month-old non-fasted female RTSAKO mice in comparison to their littermate controls do not differ in body weight. However, RTSAKO kidney weights are significantly greater, which is presumed to be due, at least in part, to increased storage of TAG as a result of a non-functional ATGL enzyme in the epithelial cells of proximal and distal renal tubules (fig.3b). Since the kidneys account for only about 2-5% of the overall body weight, an increase in kidney weight is not typically substantial enough to cause changes to body weights. Analysis of other organs such as the liver, pancreas, heart, skeletal muscle and adipose tissue (brown, retroperitoneal, inguinal, perirenal, and gonadal) indicated these were all similar in weights between the RTSAKO mice and their control littermates.

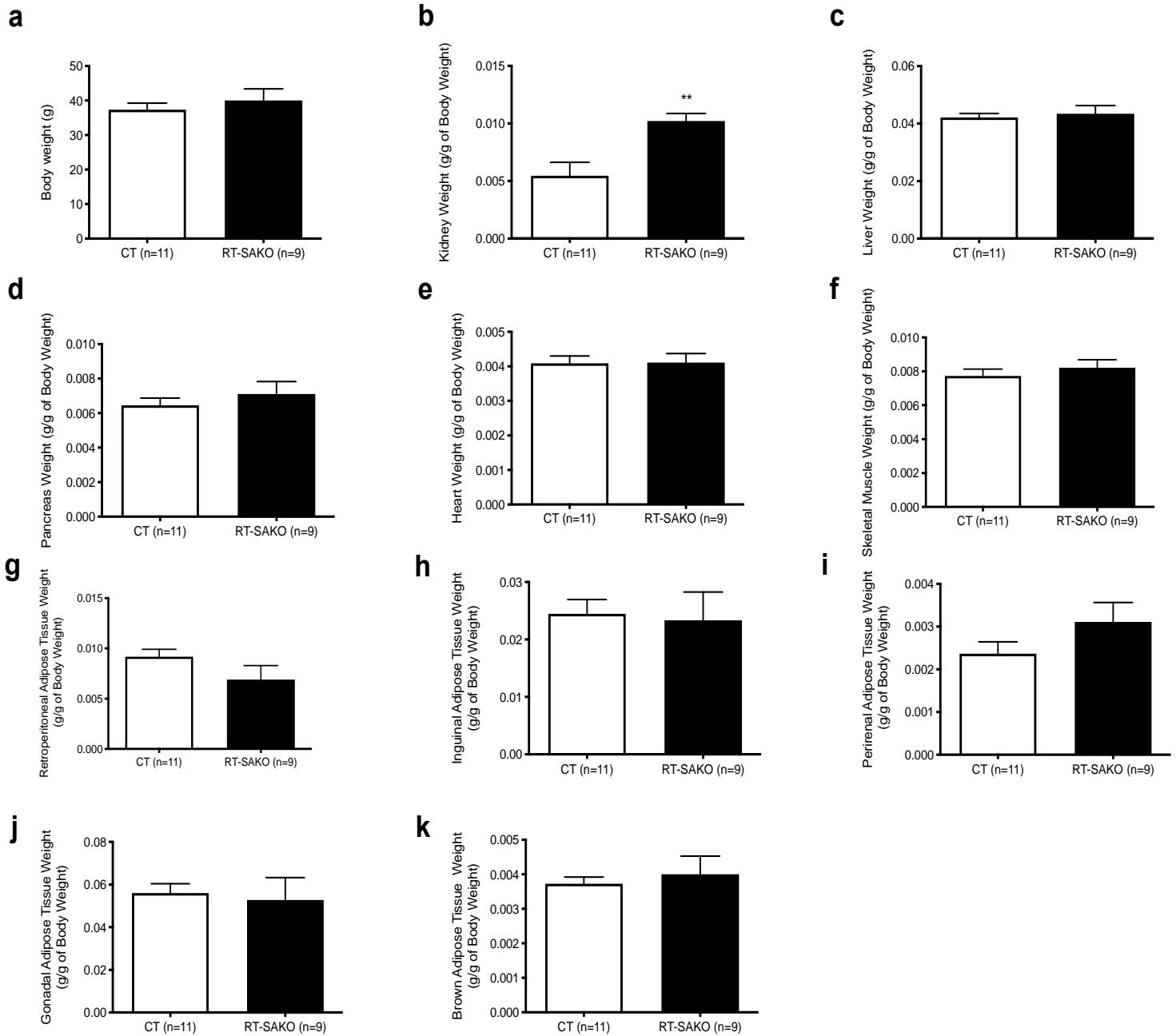


Figure 3: Body and Organs Weights of Control (CT) and Knockout (RTSAKO) mice
 (a) Body weights. (b-k) Tissues and organs from mice aged 14 – 16 months were harvested and weighed. The results are normalized to body weight (n = 9-11). Mice were euthanized, and tissues collected, while in the non-fasted state. An unpaired t-test was conducted, **P<0.01.

Lipolysis and Lipogenesis: The mRNA expression of *Hsl*, *Dgat1*, and *Lipin1* were not significantly different between the 14-16-month old female RTSAKO mice and control littermates, suggesting a lack of compensatory effects on lipid metabolism in RTSAKO mice kidneys, at least at the level of gene expression.

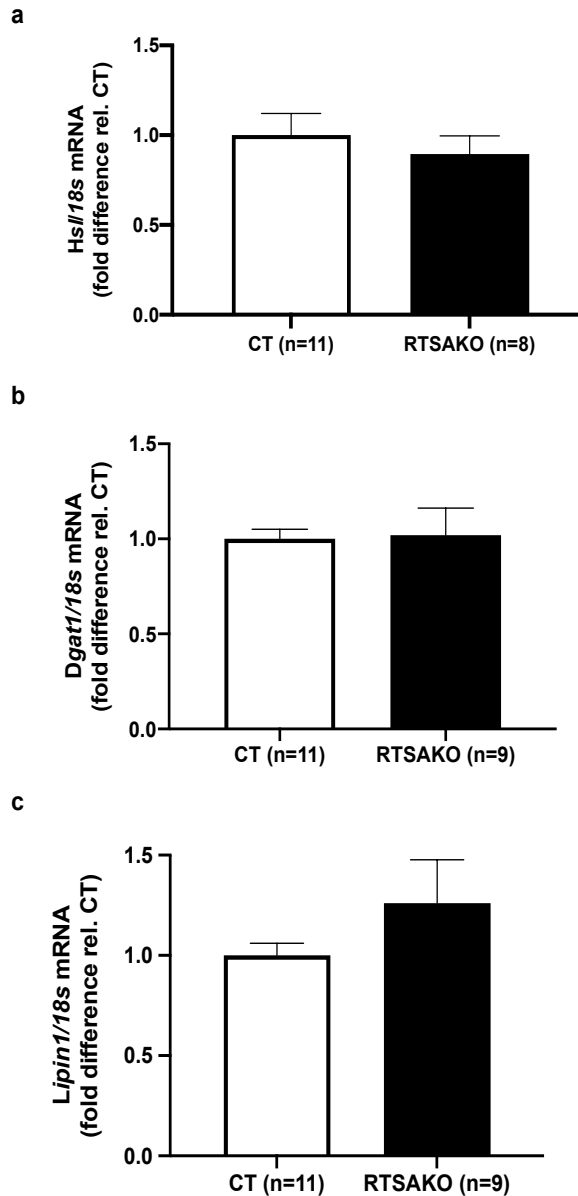


Figure 4: Renal expression of *Hsl*, *Dgat1*, and *Lipin 1*

(a) *Hsl*, (b) *Dgat1*, (c) and *Lipin1* mRNA expression are shown. Gene expression was first normalized to *18s* as an internal control, and then expressed relative to expression of the same gene by littermate controls.

Inflammation: The mRNA expression of *Tnfa*, *Il-1 β* and *Il-6* were analyzed in kidneys of 14-16-month-old female RTSAKO mice, and no significant differences were observed.

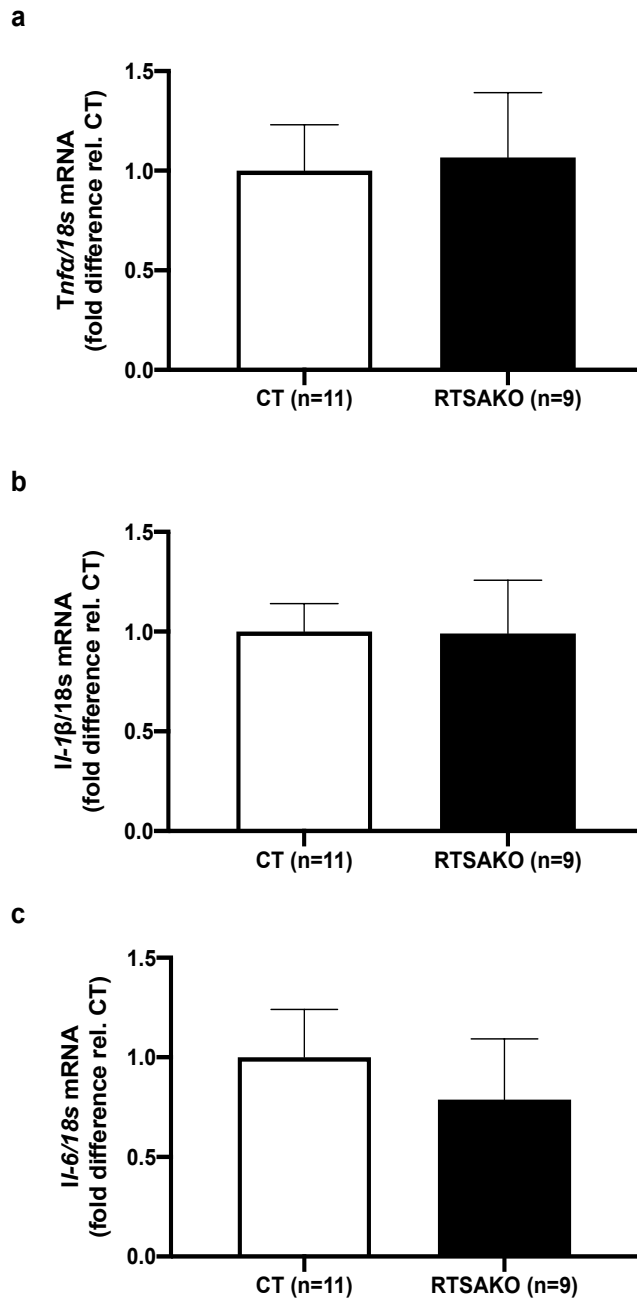


Figure 5: Expression of Genes Implicated in Inflammation in Kidneys of Control (CT) and Knockout (RTSAKO) mice

(a) Tumour Necrosis Factor alpha (*Tnfa*), (b) Interleukin 1 beta (*Il-1 β*), and (c) Interleukin-6 (*Il-6*) mRNA expression. Gene expression was first normalized to *18s* as an internal control, and then expressed relative to expression of the same gene by littermate controls (CT).

Fibrosis: To evaluate fibrosis, the expression of *Colla1*, *Col4a1*, and *Fn-1* were assessed in 14-16-month old female RTSAKO and control mice, but no significant differences were observed between RTSAKO and control littermates.

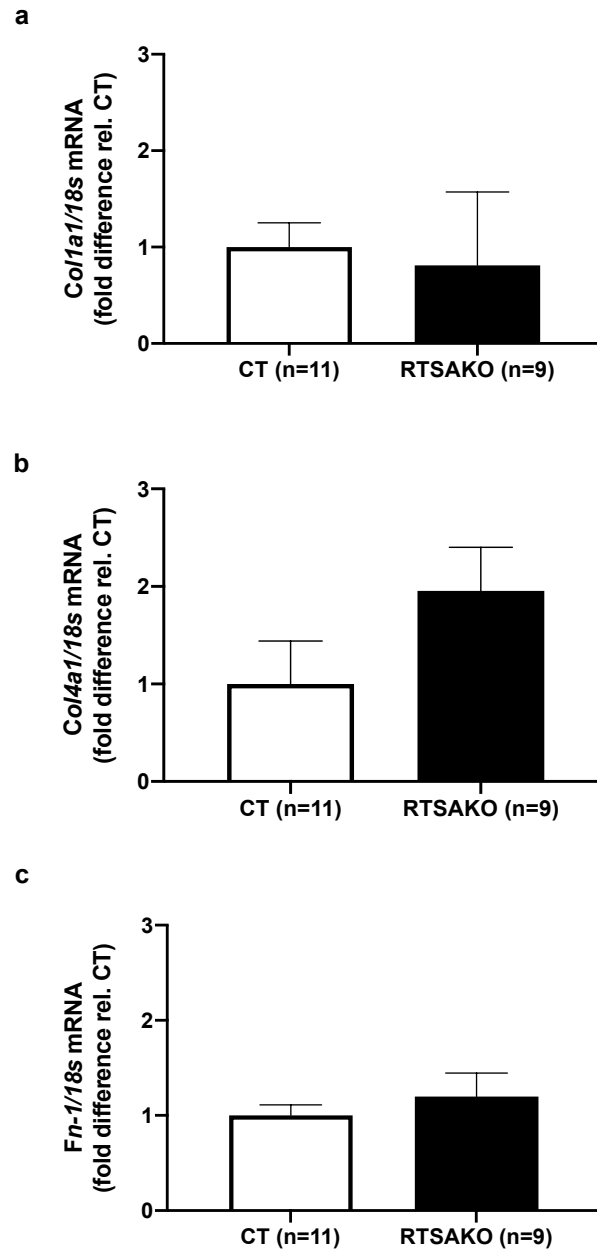


Figure 6: Expression of Genes Implicated in Fibrosis

(a) Collagen type 1 alpha 1 (*Colla1*) mRNA expression, (b) Collagen type 4 alpha 1 (*Col4a1*) mRNA expression, (c) Fibronectin 1 (*Fn-1*) mRNA expression. Gene expression was first normalized to *18s* as an internal control, and then expressed relative to expression of the same gene by littermate controls (CT).

Proliferation: Gene expression of the proliferation markers *Ki67* and *Pcna* were analyzed in 14-16-month old female RTSAKO and control mice. A small but significant increase in *Pcna* mRNA was detected in RTSAKO mice in comparison to littermate controls.

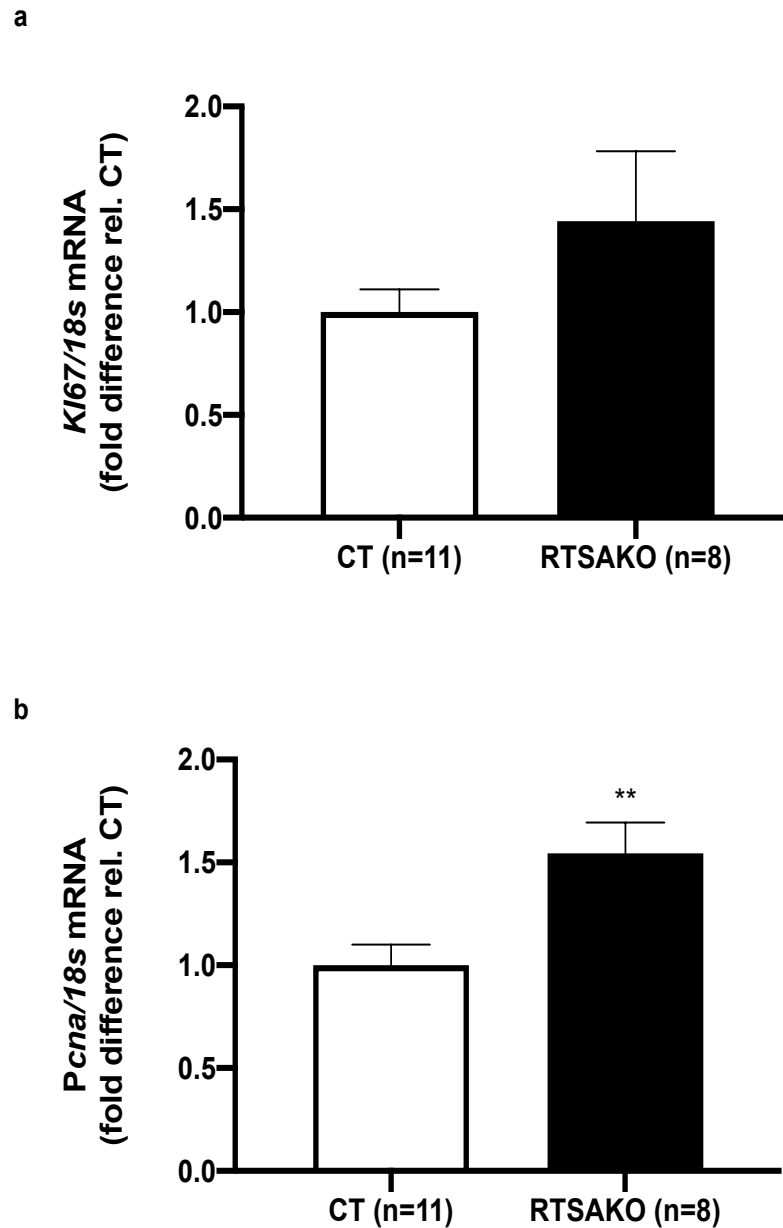


Figure 7: Expression of Proliferation Regulation Genes

(a) *Ki67* mRNA expression, (b) Proliferating cell nuclear antigen (*Pcna*) mRNA expression. ** $P < 0.01$. Gene expression was first normalized to *18s* as an internal control, and then expressed relative to expression of the same gene by littermate controls (CT).

Discussion:

The RTSAKO mouse model used by the Lipid Enzyme Discovery Lab has been genetically engineered using the Cre-Lox P system, which allows generation of tissue specific knockouts. The orientation of the Lox-P sites and the presence of Cre-recombinase determines the outcome of the genetic sequence that lies in between [72]. In our RTSAKO mice, the Lox-P sites are oriented in the same direction and the expression of Cre-recombinase is regulated by a Ksp promoter [72, 83]. Therefore, exon 1 of the genetic sequence encoding for *Atgl* is deleted in renal tubule cells, resulting in a non-functional enzyme. The specificity of our approach was validated by the finding that the expression of *Cre* is only evident in the kidney, and not in liver, brain, skeletal muscle, heart, or pancreas.

The RTSAKO mouse model provides an opportunity to examine changes resulting from renal tubule-specific loss of *Atgl*. In an initial characterization study, body weights and tissue masses were examined. RTSAKO mice did not differ significantly in body mass from their control littermates. Following cervical dislocation, ten different organs were harvested and weighed: kidney, liver, pancreas, heart, skeletal muscle, brown adipose tissue, retroperitoneal adipose tissue, inguinal adipose tissue, perirenal adipose tissue, and gonadal fat. After organ weights were normalized to body weights, it was evident that the kidneys of the RTSAKO mice weighed significantly more than those of the control littermates. Such a weight difference may reflect elevated renal ectopic lipid accumulation in RTSAKO kidneys due to non-functional renal tubule ATGL enzyme. Notably, this did not change body weights, since the kidneys only account for 2-5% of body weight and, therefore, an increase in kidney weight is not substantial enough to alter body weight [84]. With the exception of the kidney, other organs examined showed no significant differences between the RTSAKO mice and their control littermates. Thus, these

initial studies establish the kidney-specific nature of the 14-16-month-old female RTSAKO mouse genetic model.

A non-functional ATGL enzyme in the epithelial cells of the proximal and distal renal tubules of the RTSAKO mice is predicted to result in impaired breakdown of TAG, that could result in accumulation of this lipid. Although TAG content has not yet been measured, the larger kidney weights suggest that renal steatosis has developed, and follow-up studies are planned to assess this directly. Clinically and experimentally, renal steatosis can be observed using magnetic resonance imaging (MRI) [70], immunohistochemical staining of kidney sections [85] or through the direct quantification of renal TAG content following extraction of total lipid by the Folch method, and separation and isolation using thin layer chromatography (TLC) [86, 87]. Although, quantifying renal TAG content was an objective of this study, due to the closure of the laboratory during the COVID-19 pandemic, this measure was deferred and will be completed as a follow-up study. These data need to be added for future publication of these results.

The long-term implications of altered renal lipolysis and likely steatosis on kidney metabolism and health have not yet been reported. We first analyzed whether gene expression of enzymes related to lipolysis and lipogenesis were altered, but did not find any evidence of differences between the genetic strains. Measures of *Hsl* total and phosphorylated protein levels, as well as protein levels of the lipid synthesis enzymes *Dgat1* and *Lipin1*, would augment understanding of whether compensatory changes had, indeed, occurred in renal tubule cells. In addition, future studies should examine the gene expression of MAG, since increased levels may contribute to the production of MAG synthesis that is a substrate for LPA synthesis via an acylglycerol kinase [31].

Since prolonged lipid overstorage utilization may cause lipotoxicity that is not evident in younger mice, the expression of genes involved in inflammation, fibrosis and proliferation (for organellar repair) were also analyzed. To assess inflammation, mRNA expression of *Tnf α* , *Il-1 β* and *Il-6* were used, since these cytokines are most commonly produced during acute inflammation [88-90]. Fibrosis, a feature of many inflammatory diseases, is defined by scarring due to the build-up of extracellular matrix (ECM) components which overtime leads to organ malfunction and subsequent death [91]. Collagen is the primary component of the ECM, and the 28 members of this protein family collectively aid in making up the ECM of various tissues in the body [92]. To evaluate fibrosis, *Colla1*, *Col4a1* and *Fn-1* were analyzed. *Colla1*, a type I collagen, is predominately found in connective and embryonic tissue, whereas, *Col4a1*, a type IV collagen, is the main collagen component of the basement membrane of epithelial and endothelial cells [93, 94]. *Fn-1* is shown to aid in the formation of the ECM, and creates fibers to assist in tissue repair proceeding injury [95].

There was no significant difference in the expression of any of the genes analyzed as markers of fibrosis or inflammation. Since these pathways are transcriptionally controlled [74], this strongly suggests that the degree of fibrosis and inflammation is largely similar in female RTSAKO mice at 14-16 months of age relative to control littermates. It is possible that very mild damage does occur as a result of renal tubule steatosis, but that this is repaired by the proliferation of renal stem cells in a manner that does not elicit the infiltration of immunocytes or the development of fibrosis, and this is supported by the finding of increased *Pcna* expression [96]. Indeed, because the kidneys participate in the concentration and removal of toxins, and therefore are subjected to chronic high levels of damage, efficient repair and cell replacement mechanisms are present [18, 96]. Regardless, it was still surprising to find so few differences in

expression of genes related to health and metabolic markers in kidneys of aged female RTSAKO mice.

Taken together, these studies characterizing the basic phenotype of 14-16-month-old female RTSAKO mice validate the kidney-specific nature of this gene knockout model. Furthermore, this work demonstrates that although the kidneys of these mice are enlarged, suggesting renal steatosis, they are relatively healthy, without overt evidence of lipotoxicity, inflammation, or fibrosis. This background assessment of the model is important as a basis for understanding results from additional studies on the metabolic phenotype of these mice.

Chapter 4: Studies on Glucose Tolerance and Insulin Sensitivity in 14-16-Month-Old Female RTSAGO Mice

Rationale: The ability of the kidney to modulate blood glucose through the absorption, secretion and de novo synthesis of glucose causes it to play a direct role in regulating whole-body glucose metabolism and homeostasis [18, 19]. Prior unpublished work from our laboratory has also demonstrated that altering renal lipolysis in young male, but not female RTSAGO mice can indirectly alter glycemic control, by modulating the production of LPA by the kidneys. This elevated LPA is secreted into blood, where it serves to inhibit insulin secretion, and therefore impair glycemic control (unpublished data). Importantly, this occurs without any evidence of altered glucose handling by the kidneys, strongly suggesting that this indirect regulatory effect by LPA is the major mechanism underlying impaired glycemic control in young male RTSAGO mice (unpublished data).

In the case of our RTSAGO mice, we sought to determine if female mice at an older age develop similar alterations in glycemic control to those observed in young male RTSAGO mice. In preliminary studies, our laboratory has found that female RTSAGO mice at 6 months of age do not display impaired glucose tolerance (unpublished observation, data not shown), and we therefore hypothesized that female mice, like human women, may have a longer latency and therefore may, with time, develop similar metabolic complications. Thus, I have investigated glucose tolerance and insulin resistance in female RTSAGO mice that are 14-16 months old. In that work, reported in this chapter, I found evidence of impaired glucose tolerance, without alterations in insulin sensitivity, that recapitulates the phenotype of young male RTSAGO mice. To better understand our findings from this work, I examined levels of hormones related to glucose disposal, including insulin, resistin, leptin, and glucagon. Although it was not possible in

this thesis to examine concentrations of LPA in the blood or kidneys, testing for a protective effect of the LPA-receptor inhibitor Ki16425 during glucose tolerance testing was used to infer a likely role for LPA in mediating differences in glycemic control between RTSAKO and control littermates.

Objectives:

1. To determine glucose tolerance and insulin sensitivity, and blood concentrations of hormones related to these measures, in 14-16-month-old female RTSAKO mice and control littermates.
2. To investigate a potential role for Ki16425 in restoring the impaired glucose control in 14-16-month-old female RTSAKO mice.

Hypotheses:

1. Female RTSAKO mice will develop impaired glucose tolerance at 14-16 months of age. Insulin sensitivity will not differ between genotypes. Serum insulin concentrations will be lower, while levels of resistin, leptin and glucagon will not be different.
2. Ki16425 will restore glucose tolerance in female RTSAKO mice (age 14-16 months), supporting a likely role for increased circulating LPA concentrations in the impaired glucose tolerance observed.

Methods:

Study Design

All protocols were approved by the Animal Care Committee at the University of Waterloo (AUPP#30053). The mice were kept at the Central Animal Facility at the University of Waterloo in group housing with a chow diet and water. The conditions in which they are housed are controlled to a 12h hour dark and light cycle with constant temperature. Female RTSKO and control mice age 14-16 months will be used for this study.

Glucose Tolerance Test

Mice were single housed and fasted overnight for 12 hours. Following fasting the weight of each mouse was measured and recorded to administer a weight-dependent dosage (1 unit (U) or 0.01 mL to 1 gram of body weight) of freshly prepared 20% glucose solution [97, 98]. A sterile 1 mL 25-gauge syringe was used to administer the solution via an *intraperitoneal* (*i.p.*) injection. Blood glucose was measured using a FreeStyle Lite® glucose monitor with an ~2µL blood sample obtained from the mouse tail. Readings were taken at 7 timepoints: 0, 7, 15, 30, 60, 90 and 120mins following the *i.p.* glucose injection [97].

Insulin Tolerance Test

Mice were single housed overnight and provided with control chow diet and water. Diet was removed ~1-2 hours prior to testing, and body weight of each mouse was measured immediately prior to testing in order to administer a 0.1 U/mL solution of Insulin dissolved in sterile 1 × Phosphate-buffered saline (PBS) solution. A 1 mL 25-gauge syringe was used to administer 0.5 U of insulin per kilogram of bodyweight via an *i.p.* injection [98]. Blood glucose was measured using a FreeStyle Lite® glucose monitor with an ~2µL blood sample obtained

from the mouse tail. Readings were taken at 6 timepoints: 0, 15, 30, 60, 90 and 120mins following the *i.p* glucose injection [98].

Ki16425 Injection

The protocol was as described by Rancole et al., where the Ki16425 prepared at 1mg/mL was administered to mice at a dose of 5 mg/kg. The injection given was followed by a glucose tolerance test 30 minutes later, and blood glucose readings were taken at 7 timepoints: 0, 7, 15, 30, 60, 90 and 120mins following the injection with glucose [55].

Bio-plex – Hormonal analysis

Mice were euthanized by cervical dislocation. An incision was immediately made near the thoracic cavity to expose the chest area and heart for blood collection. A sterile 1 mL 25-gauge syringe is inserted into the right atrium to draw approximately 300 μ L of blood. The blood was placed in a 1.5mL microfuge tube at room temperature for a minimum of 30 minutes to coagulate. After 30 minutes, the tubes were placed in a centrifuge at 4°C for 10 minutes at 3000 rcf. The serum was pipetted into new sterile 1.5mL microfuge tubes and stored at -80°C. Serum was assayed using a Bio-Plex ® (Bio-Rad) Pro Mouse Diabetes immunoassay (catalogue #171F7001M) which is a 96-well kit containing detection antibodies and diluents, 6.5 μ m magnetic beads, standards, buffers and streptavidin-PE, that detects and quantifies hormones related to diabetes development, including glucagon, insulin, leptin, and resistin [99]. This assay uses the xMAP technology, which allows approx. 100 different assays to be completed using a single sample [100]. The technique uses an array of colored bead sets that is created by varying ratios of two fluorescent dyes [100]. Here, two antibodies, one with a particular color bead and another with a fluorescent reporter dye label is attached and surrounds the analyte [100]. Using different color beads allows simultaneous detection of multiple analytes in one sample [100]. As

well, a dual detection flow cytometer is used [100]. One channels recognizes different assay beads by color, while the other channel determines the analyte concentration by measuring the fluorescence of the reporter dye [100]. The data is then processed using an array reader [100]. For this study, the assay was operated by a technician in the pathobiology laboratory of Dr. Geoffrey Wood at the University of Guelph, and output results were processed by Dr. Fernandes as part of a larger cohort of experimental mice.

Mice Used

Cohort 1	
Control	RTSAKO
67 2-2	64 2-1
67 2-3	64 2-2
68 2-2	64 2-3
69 2-1	64 2-4
69 2-2	65 2-1
69 2-5	65 2-3
70 2-1	66 2-1
72 2-1	66 2-3
72 2-3	67 2-1
72 2-4	
73 2-1	

CT n=11
RTSAKO n=9

Age at the time of experiment:
14 months

Cohort 2	
Control	RTSAKO
168 2-2	167 2-3
169 2-2	167 2-4
169 3-1	169 3-2
172 2-3	171 1-1
172 2-5	171 1-2
175 1-2	181 2-4
173 2-2	182 2-1
167 2-3	182 2-2
	167 2-1
	169 3-3

CT n=8
RTSAKO n=10

Age at the time of experiment:
15-16 months

Statistical Analysis

Statistical significance between groups of mice was assessed using the Student's *t* test and planned comparisons, where specific timepoints and area under the curve (AUC) for GTT (timepoint 0, 7, 15, 30, 60, 90 and 120 min) and ITT (timepoints 0, 15, 30, 60, 90 and 120 min) were planned for measurement and comparison *a priori* between the control (CT) and knockout (RTSAKO) mice. In addition, one-way ANOVA with Tukey's post-hoc test was performed to determine whether insulin or glucose administration caused significant excursions from baseline in blood glucose, to validate the successful application of the tests, and to identify the timepoint when blood glucose was no longer different from baseline. Results are expressed as the mean +/- standard error of the mean (S.E.M). A P-value of <0.05 was deemed significant.

Results:

Glucose Tolerance: Glucose tolerance testing was performed on 14-16-month-old female RTSAKO and control mice (Fig. 8a). Both groups of mice began at similar blood glucose concentrations of approximately 4.2 mmol/L, and analysis of the individual response curves within genotypes indicated that mice responded to glucose administration with significant elevations in blood glucose. However, following the glucose injection of 2.0 g/kg of body weight, the mean blood glucose concentration of RTSAKO mice was significantly higher than the mean concentration of littermate controls, when measured at the 7-minute timepoint. Throughout the remainder of the 120-minute experiment, no other individual timepoints were found to be statistically significantly different. However, the mean blood glucose concentrations of RTSAKO mice, overall, remained marginally elevated, as demonstrated in fig. 8b, as differences in the mean areas under the curve for each genetic group ($p < 0.05$). The control mice returned to baseline glucose concentration at an earlier timepoint than RTSAKO mice, although RTSAKO mice did return to baseline by the end of the 120-minute trial. Therefore, the RTSAKO mice display glucose intolerance when compared to the control mice.

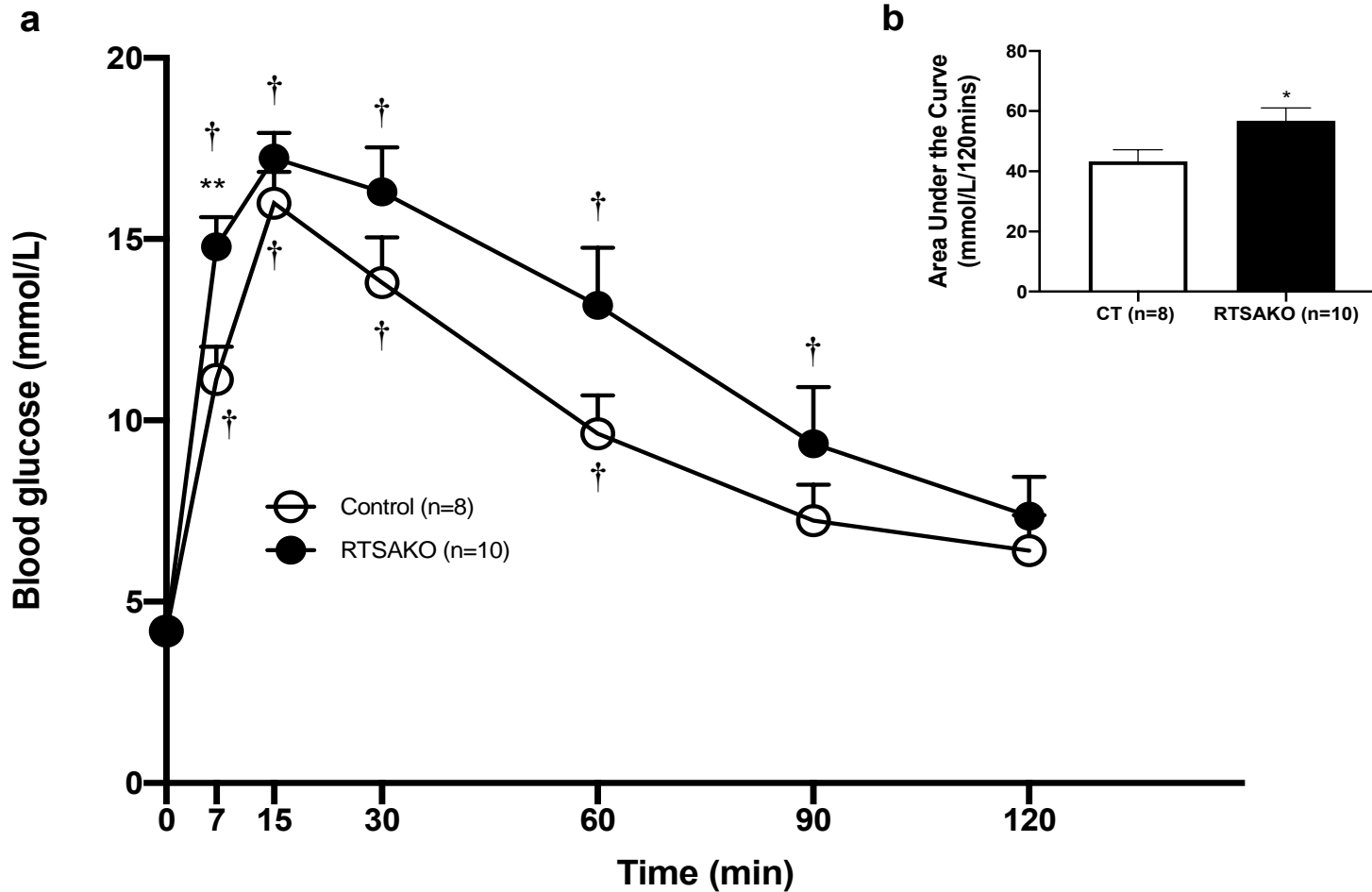


Figure 8: Glucose Tolerance Testing in Control (CT) and Knockout (RTSAKO) mice

(a) Blood glucose was monitored at timepoints 0, 7, 15, 30, 60, 90 and 120 min using a blood glucose meter. An unpaired t-test at all 7 timepoints was used to compare responses between control and RTSAKO mice. ** $P < 0.01$. One-way Anova with Tukey's post-hoc test was performed to compare blood glucose measures at different timepoints within each genotype to timepoint 0. † $P < 0.05$ versus timepoint 0 mins. b) The AUCs were compared using an unpaired t-test and showed a significant difference between the control and RTSAKO mice. * $P < 0.05$.

Insulin Sensitivity: Insulin sensitivity testing was performed on 14-16-month-old female RTSAKO and control mice. The control and RTSAKO mice had initial blood glucose concentrations of 6.80 and 7.1 mmol/L, respectively (fig. 9a). After an insulin injection of 0.5 U/kg of body weight was administered, there was an overall decrease in blood glucose in both the RTSAKO and control mice, indicating insulin responsiveness at the dose administered. Throughout the 120-minute experiment, both groups responded, overall, in a similar manner, and there were no significant differences between blood glucose concentrations at any of the *a priori* chosen timepoints (fig. 9a). As depicted in figure 9b, area under the curve analysis indicates that there was no significant difference across the experiment in the response between mice with different genotypes. Therefore, both the RTSAKO and control mice largely respond in a similar manner to exogenous insulin and therefore both groups are similarly insulin sensitive.

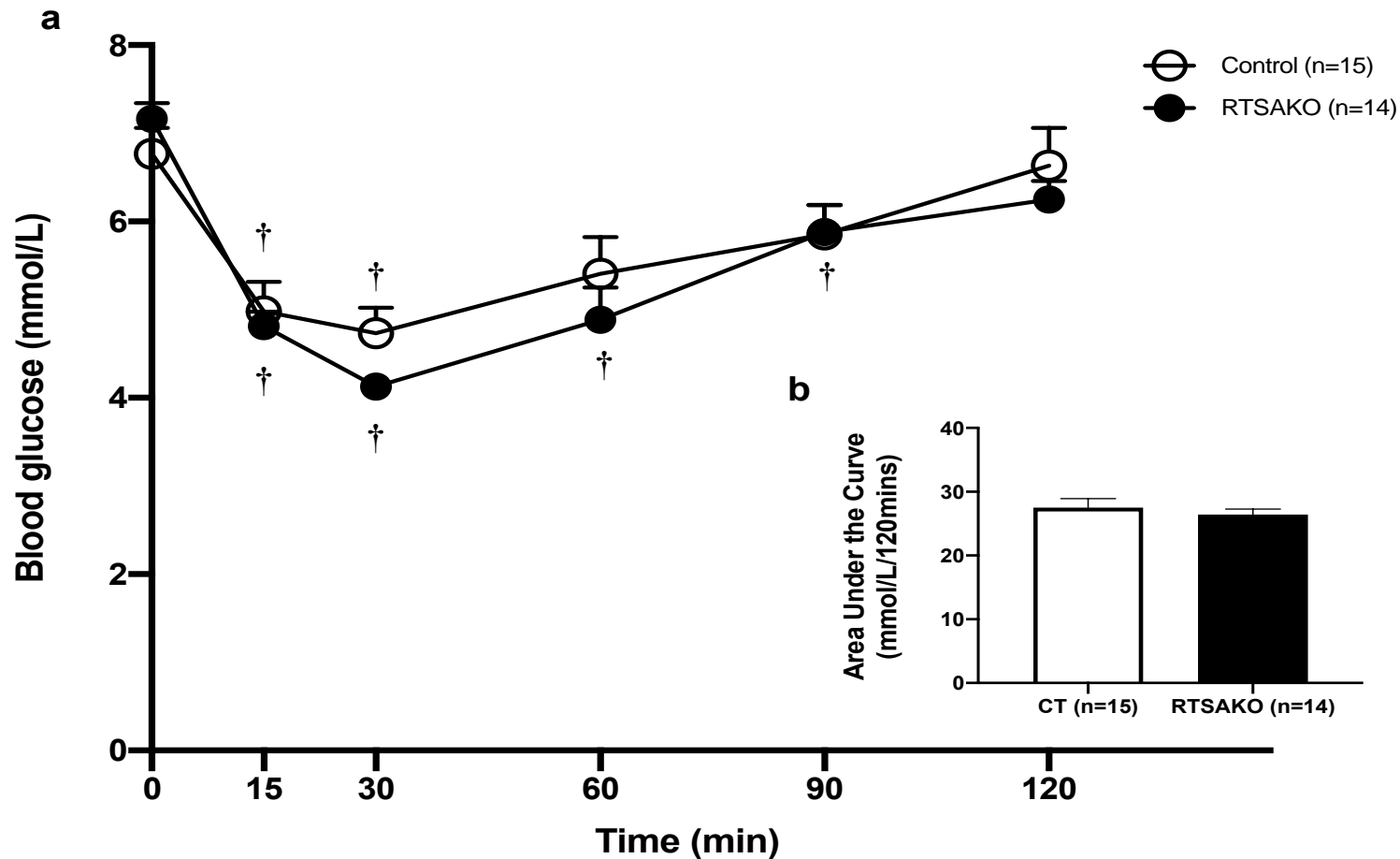


Figure 9: Insulin Tolerance Testing in Control (CT) and Knockout (RTSAKO) mice

(a) Blood glucose was monitored at timepoints 0, 15, 30, 60, 90 and 120 min using a blood glucose meter. One-way Anova with Tukey's post-hoc test was conducted, demonstrating that animals exhibited a significant response to insulin. However, unpaired t-tests between planned timepoint comparisons (0, 15, 30, 60, 90 and 120 min) demonstrated no difference between the control and RTSAKO mice. †P<0.05 versus blood glucose measures in animals with the same genotype at timepoint 0 mins. B) The AUC was calculated using an unpaired t-test and was not significantly different between genotypes. *P<0.05.

Glucoregulatory Hormones: Biomarkers of glucose regulation were investigated: glucagon, insulin, leptin and resistin in the 14-16-month-old female RTSAKO mice. The results were processed by Dr. Fernandes as part of a larger cohort of experimental mice and analyzed using an unpaired t-test. Serum levels of leptin, resistin, and glucagon did not differ significantly between RTSAKO and control littermate mice. Serum levels of insulin were significantly lower, by ~40%, in RTSAKO mice than in littermate controls.

Table 7: Bio-plex Hormone Assay

<i>Hormone</i>	<i>Mean (pg/mL)</i> <i>± S.E.M.</i>		<i>P-Value</i>
	<i>Control (n=5)</i>	<i>RTSAKO (n=5)</i>	
<i>Glucagon</i>	180.2 ± 22.3	221.5 ± 19.86	0.20
<i>Insulin</i>	202.2 ± 16.69	119.0 ± 17.91	<0.01
<i>Leptin</i>	155.2 ± 13.19	211.5 31.91	0.14
<i>Resistin</i>	198610 ± 8128	230340 ± 22062	0.21

Ki16425 Rescue: The Ki16425 rescue was performed on 14 – 16-month-old female RTSAKO mice and their control littermates. Thirty minutes after the pre-treatment with Ki16425, glucose was administered at a dose of 2.0 g/kg of body weight. Following the Ki16425 injections, the RTSAKO mice and control littermates had an approximate blood glucose concentration of 5.2 mmol/L. Both groups of mice responded to the glucose challenge, demonstrating a significant increase in blood glucose concentrations after injection. As depicted in fig. 10a, throughout the 120-minute experiment, both groups of mice had similar blood glucose concentrations, with no significant differences at any of the timepoints examined. According to the area under the curve analysis (fig. 10b), the 14-16-month-old female RTSAKO mice and their control littermates had comparable blood glucose levels, indicating that the overall response was highly similar between genotypes.

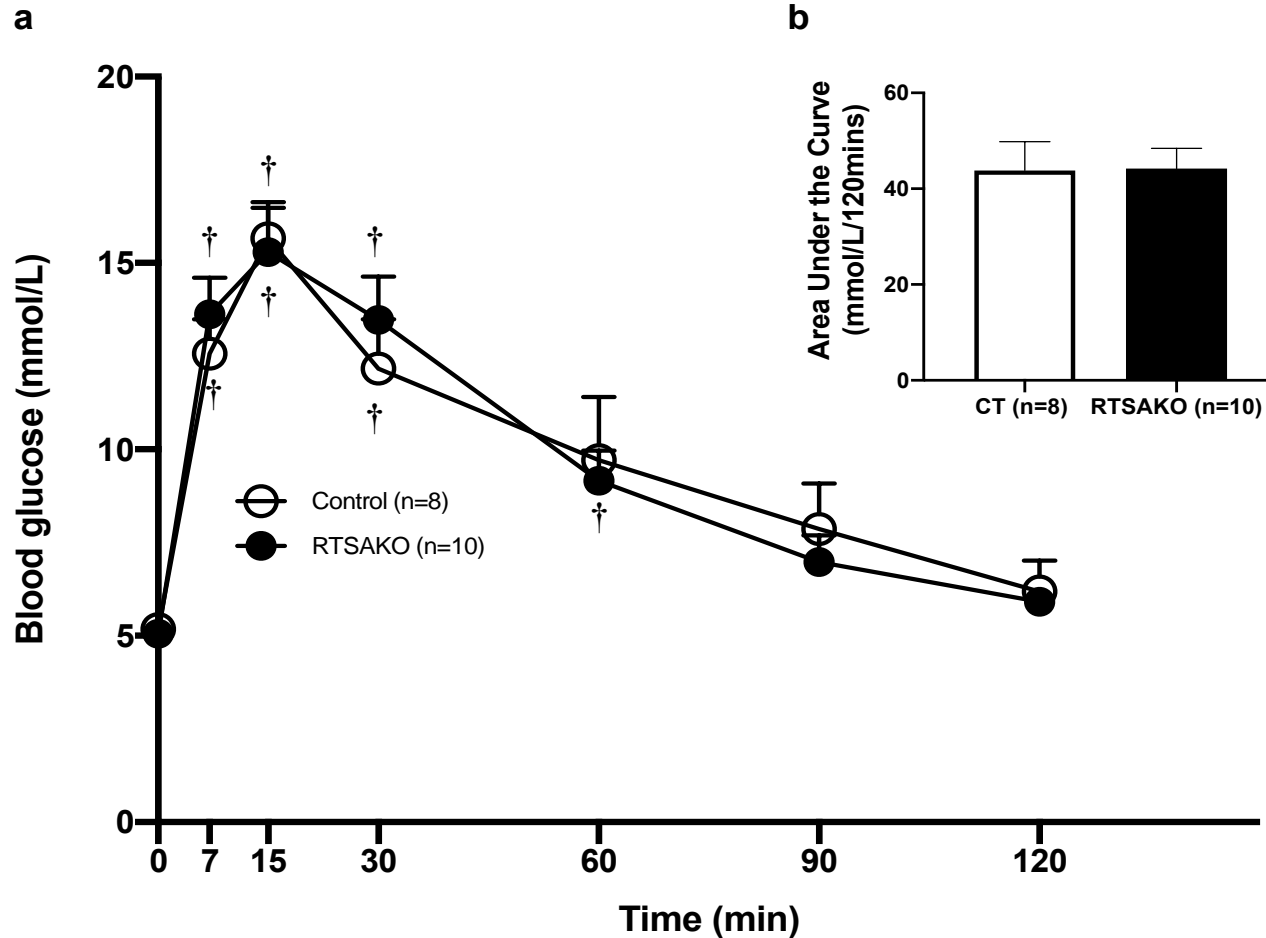


Figure 10: Glucose tolerance of RTSAKO mice and control (CT) littermates following Ki16425 Pre-treatment

(a) Blood glucose was monitored at timepoints 0, 7, 15, 30, 60, 90 and 120 min using a blood glucose meter. One-way ANOVA with Tukey's post-hoc test was performed to compare timepoint blood glucose measures within each genotype to timepoint 0, to confirm that glucose injection caused an increase in blood glucose. †P <0.05 versus timepoint 0 mins. Unpaired t-tests comparing control and RTSAKO mice at planned timepoints (0, 7, 15, 30, 60, 90 and 120 min) demonstrated no significant differences between the genotypes at any single timepoint. b) The AUC was calculated and compared between genotypes using an unpaired t-test and was found not to be significantly different. *P<0.05.

Discussion: Glucose and insulin tolerance testing in female RTSAKO mice by other members of our laboratory at 9-10 weeks, 16-18 weeks, and 4 and 6 months of age, have indicated that females are both glucose and insulin sensitive, unlike their male counterparts that develop glucose intolerance at 16-18 weeks of age. The primary objective of this study was therefore to investigate whether aged female RTSAKO mice develop this same glucose intolerance with advancing age. It was hypothesized that such metabolic alterations accompany older age in female RTSAKO mice, because similar trends are present in human women that manifest chronic diseases nearly 10 years later than men [27].

Conducting glucose tolerance testing (GTT) on the 14-16-month-old female RTSAKO mice indicated that they are glucose intolerant in comparison to their control littermates. During GTT, a bolus of glucose is injected intraperitoneally. In doing so, the body should ideally respond to the excess blood glucose by releasing insulin to stimulate insulin-mediated glucose uptake by skeletal muscle and adipose, and to suppress hepatic gluconeogenesis [13, 58, 59]. However, in the case of our RTSAKO mice, the data suggest a likely deficiency in insulin secretion following glucose administration, since responsiveness to insulin was not impaired. Interestingly, at the 7-minute timepoint, it is evident that the control mice have a better physiological response to exogenous glucose than the RTSAKO mice, suggesting that early phase insulin secretion specifically, may be impaired. Similarly, because blood glucose concentrations in both RTSAKO and control mice returned to levels that were not significantly different from baseline by 120 minutes, this suggests that the later phase of insulin secretion was less affected than the early phase of secretion.

Bio-plex analysis was performed and allows for direct analysis of blood insulin concentrations, although it does not indicate blood insulin concentration in response to a glucose

challenge and cannot be used to distinguish between early and late phase insulin secretory responses. Notably, baseline blood insulin concentrations in RTSAKO mice were lower than measures in control littermates, suggesting impaired insulin secretion. Further studies measuring blood insulin levels following glucose administration should be performed to assess early and late phase insulin secretion. The Bio-plex results also allow for comparison of a variety of adipocyte- and pancreas-derived hormones that play roles in glucose regulation. In agreement with findings that adipose tissue masses and insulin sensitivity were not altered, there were no differences between RTSAKO and control littermates in leptin or resistin concentrations. Glucagon levels were also not different, which aligns with findings that the pancreatic mass of RTSAKO mice was unaltered.

Investigations by our lab, and mechanistic studies done in collaboration with the Stark lab, have previously revealed elevated plasma LPA levels in 16-18-week-old male RTSAKO mice (unpublished observation, data not shown). As a result, I hypothesized that elevated blood LPA may also mediate glucose intolerance in the female RTSAKO mice. Analysis using mass spectrophotometry to quantify plasma LPA concentrations in female RTSAKO mice could not be performed in the present study. Use of an LPAR antagonist such as Ki16425, which can block LPA-mediated signaling via the LPAR1/2/3 receptors, can be used to infer a likely role for this bioactive lipid in glucose intolerance. In the current work, pre-administration of Ki16425 caused the glucose response curves for RTSAKO and control mice to converge strongly suggesting that elevated LPA is a source of both the decreased circulating insulin detected in the Bio-plex assay, and the impaired glucose tolerance of aged female RTSAKO mice. To determine whether LPAR antagonism improved glucose disposal in RTSAKO mice relative to mice not given Ki16425 pre-treatment, studies should be repeated illustrating the response of control and RTSAKO mice

to pre-injection of the vehicle control. The vehicle control, consisting of 10% DMSO, is not expected to affect glucose tolerance. Therefore, a figure comparable to glucose tolerance testing without Ki16425 pre-treatment is expected. However, since the stress of pre-injection can, potentially, affect glycemic control, having such control results will indicate that the vehicle did not interfere in restoring the glucose intolerance, thus showing Ki16425 treatment to be solely responsible for the rescue in the 14-16-month-old female RTSAKO mice.

Chapter 5: Measures of Activity and Energy Expenditure in 14-16-month-old Female RTSAKO mice

Rationale: Energy metabolism varies widely amongst organisms [101]. The consumption of oxygen and production of carbon dioxide gives an insight into energy expenditure, while also indicating the function of tissues and organs [101]. Tools such as indirect calorimetry allow for the quantification of these variables, and knowing VO_2 and VCO_2 will allow for the indirect calculation of other factors such as heat production and respiratory exchange ratio (RER) [102]. Each metabolic variable yields specific information. For example, RER will indicate the predominate substrate being utilized, and whether there are changes in the preferred use of carbohydrates or fats [103]. Others, such as elevated VO_2 , may allow for generalized interpretations of metabolic activity [103]. These measurements are made with four specific assumptions: 1. The food consumed will undergo metabolic modification to yield either heat or energy; 2. All biochemical reactions in the body end in a synthesis or combustion of fat, protein or carbohydrates; 3. The ratio between CO_2 produced and O_2 consumed indicates the predominate substrate being utilized (glucose, fat, or protein); 4. Fecal and urinary excretion is negligible [102]. In addition, information on locomotion in the X, Y and Z direction will aid in understanding the movement pattern of RTSAKO mice and their littermate controls during the day and night when activity is the least and most, respectively [104].

RTSAKO mice are engineered with intentional changes to renal lipid metabolism, and in Chapter 4, I have found that this is associated with higher glucose and lower circulating insulin levels. Therefore, alteration to glucose metabolism may cause the RTSAKO mice to use carbohydrates as their preferred source of substrates, ultimately leading to changes in RER. Since metabolic characterization has not been performed at any age in the female RTSAKO mice, having this information will be useful in determining if metabolic differences exist

between the female RTSAKO mice and their control littermates, or whether they are largely similar.

Objective:

1. To understand whether 14 – 16-month-old female mice exhibit differences in locomotor activity or energy use and expenditure.

Hypotheses:

1. It is expected that locomotion will be the same in all directions (X, Y and Z) in the RTSAKO mice in comparison to their control littermates.
2. RER will be higher in female RTSAKO mice with no changes to VO_2 , VCO_2 and heat, since only the kidneys showed differences in mass, and the kidneys account for only ~2-5% of body mass, and use only ~10% of transported oxygen [105]. This represents a small proportion of body oxygen use and, regardless, lipid overstorage is not expected to drastically alter kidney oxygen use. Overall VO_2 , VCO_2 , and heat production are therefore not expected to change significantly in 14-16-month-old female RTSAKO mice compared to control littermates. Since lipid use by kidney as a fuel is expected to be decreased, and since increased circulating glucose may facilitate its use as a primary energetic substrate, RER is anticipated to be higher in the female RTSAKO mice in comparison to their littermates.

Methods:

Comprehensive Lab Animal Monitor System (CLAMS)

The following protocol spans 3-days. Day 1: Mice were single-housed to monitor for food intake over a 24-hour period. The system is calibrated with a gas mixture containing O₂, CO₂ and N₂ during this time [106]. Day 2: mice are removed from their home cages and placed in specialized chambers with water and food. Body weights are entered into the system to normalize all data and the experiment operates for a total of 26 hours. An hour after initiating the experiment, the system is checked for negative values or any warnings [106]. Day 3: mice are removed from their chambers and placed in their home cages. Chambers are carefully removed, cleaned and washed. Activity was measured at 28-minute intervals during the day (light) and night (dark) cycles, in three directions: total locomotion, ambulatory activity, and rearing. Oxygen consumption (VO₂), carbon dioxide production (VCO₂), respiratory exchange ratio (RER) and heat were measured also at 28-minute intervals over a 24-hour period in the metabolic chambers, where mice were provided with food and water *ad libitum*.

Food Composition

The 14-16-month-old female RTSAKO mice and control littermates were given a standard chow diet, which is a grain-based diet encompassing ground corn, soybean meal, fish meal and other animal by-products, as well various macronutrients, minerals, amino acids, vitamins and fatty acids [107, 108]. The chow diet consumed by mice at the Central Animal Facility at the University of Waterloo is the Teklad 22/5 Rodent diet from Harlan Laboratories. The Teklad 22/5 diet is a fixed formula diet that has a macronutrient composition of 40.6% carbohydrate, 22.0% crude protein and 5.5% fat, by weight [107]. The approximate calories obtained from carbohydrates, proteins and fat are 54%, 29% and 17% respectively [107].

Mice Used

Cohort 3	
Control	RTSAKO
88 2-4	84 3-4
88 3-2	84 3-5
88 3-4	87 2-1
90 3-3	88 2-5
92 2-2	89 2-2
92 2-3	90 2-2
92 2-4	90 3-1
92 2-5	91 2-1
	86 2-3

CT n=8
RTSAKO n=9

Age at the time of experiment:
15-16 months

Statistical Analysis

Statistical differences between groups of mice were assessed using the Student's t test. Results are expressed as the mean +/- standard error of the mean (S.E.M). A P value of <0.05 was deemed significant.

Results:

Food-intake: Food intake and body weight was measured in the 14-16-month-old female RTSAKO and control mice during the 24-hour acclimatization period. The results were analyzed using an unpaired t-test. As depicted, no significant differences were observed in body weight, absolute food intake or normalized food intake (fig. 11a-c).

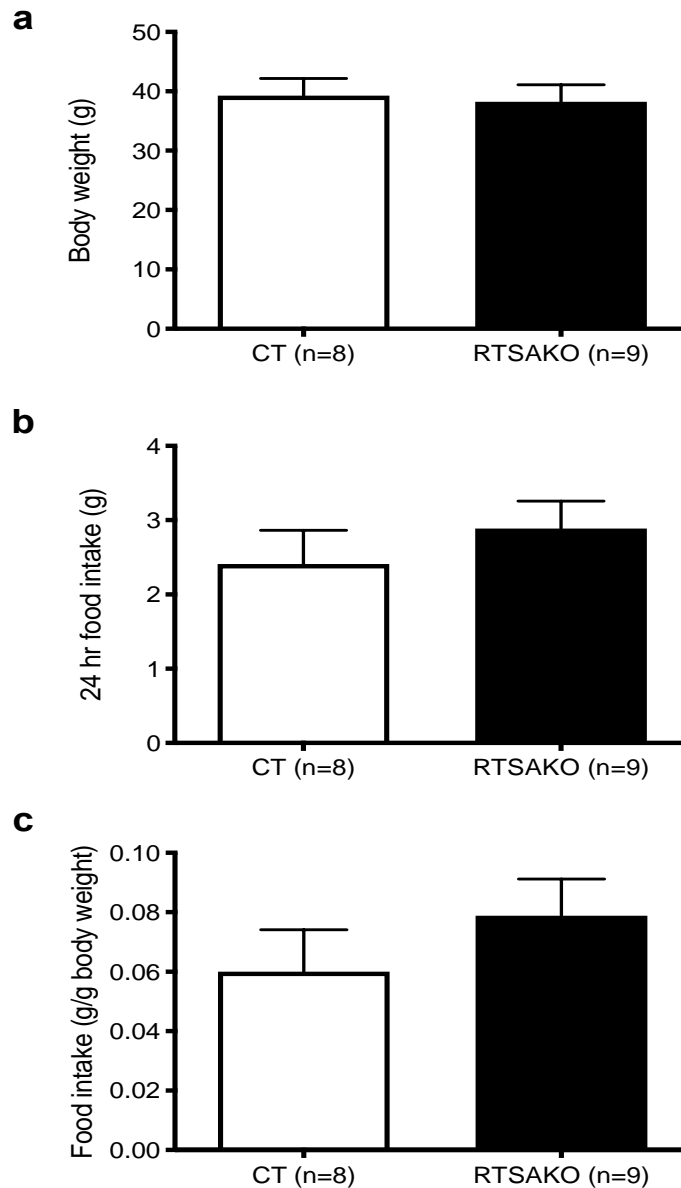


Figure 11: Food-intake and Body weight in Control (CT) and Knockout (RTSAKO) mice Food intake and body weight were measured after the 24 hours acclimatization period. (a) Body weight, (b) total 24-hour food intake, (c) food intake normalized to body weight, are presented.

Locomotion: Activity was examined in the 14-16-month-old non-fasted female RTSAKO and control mice after 24 hours in the CLAM system. The results were analyzed using an unpaired t-test. Total locomotor activity (fig.12a-c) represents the total number of infrared beams broken in either the X, Y, or Z axis directions during each of the 28-minute time intervals [109], whereas ambulatory locomotor activity (fig.12d-f) indicates when different directional infrared beams are broken (*i.e.* X or Y) [109]. For example, if the mouse is engaged in a repetitive action, such as grooming, and continuously breaks a single beam, the ambulatory count will be one until a new beam is broken [109]. Thus, horizontal movement engaging is required to activate ambulatory activity counts. Rearing locomotor activity (fig.12g-i), which is commonly referred to as movement in the Z-axis, monitors any upward activity, such as when the mouse stands on its hind legs [109]. As depicted in fig.12a-i, no significant difference in any category of activity or timeframe was identified. However, a review of the p-values generated in t-testing suggests that the study may have been underpowered.

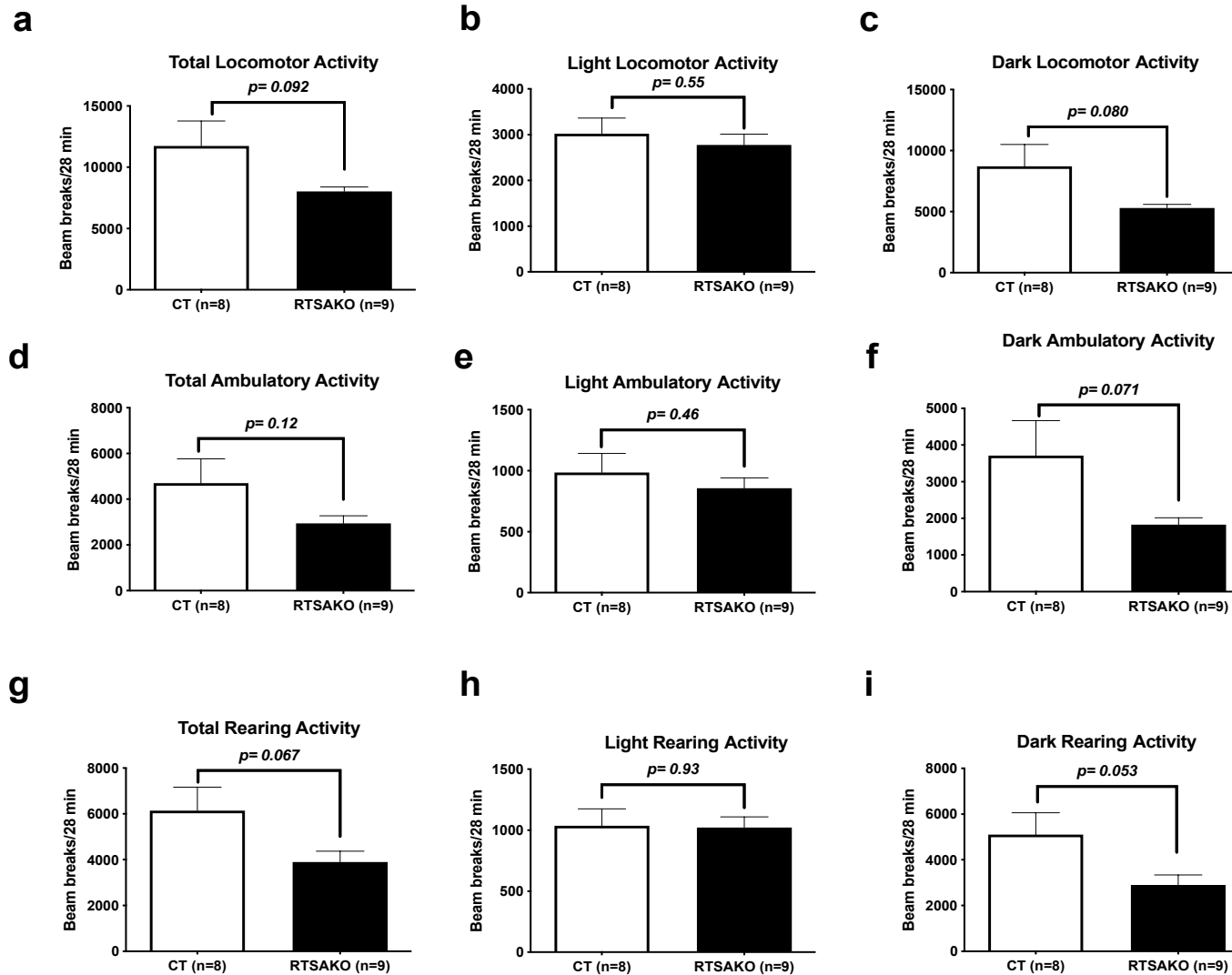


Figure 12: Activity During the Day and Night in Control (CT) and Knockout (RTSAKO) mice

Activity measured in 28-minute intervals and during the day (light) and night (dark). (a,b,c) Locomotor (all beam breaks), (d,e,f) Ambulatory (locomotor beam breaks only), (g,h,i) Rearing (Z-axis).

VO₂ Testing: The oxygen consumption of 14-16-month-old female RTSAKO and control littermate mice was analyzed using area under the curve. In fig.13a, the oxygen consumption rate over a 24-hour period, as analyzed by area under the curve (AUC), was found not to be significantly different between mice with different genotypes. When the oxygen consumption rate was analyzed across only the light or dark periods, the AUC measurements calculated for these entire periods were also not significantly different between RTSAKO and littermate controls, indicating no overall difference in VO₂.

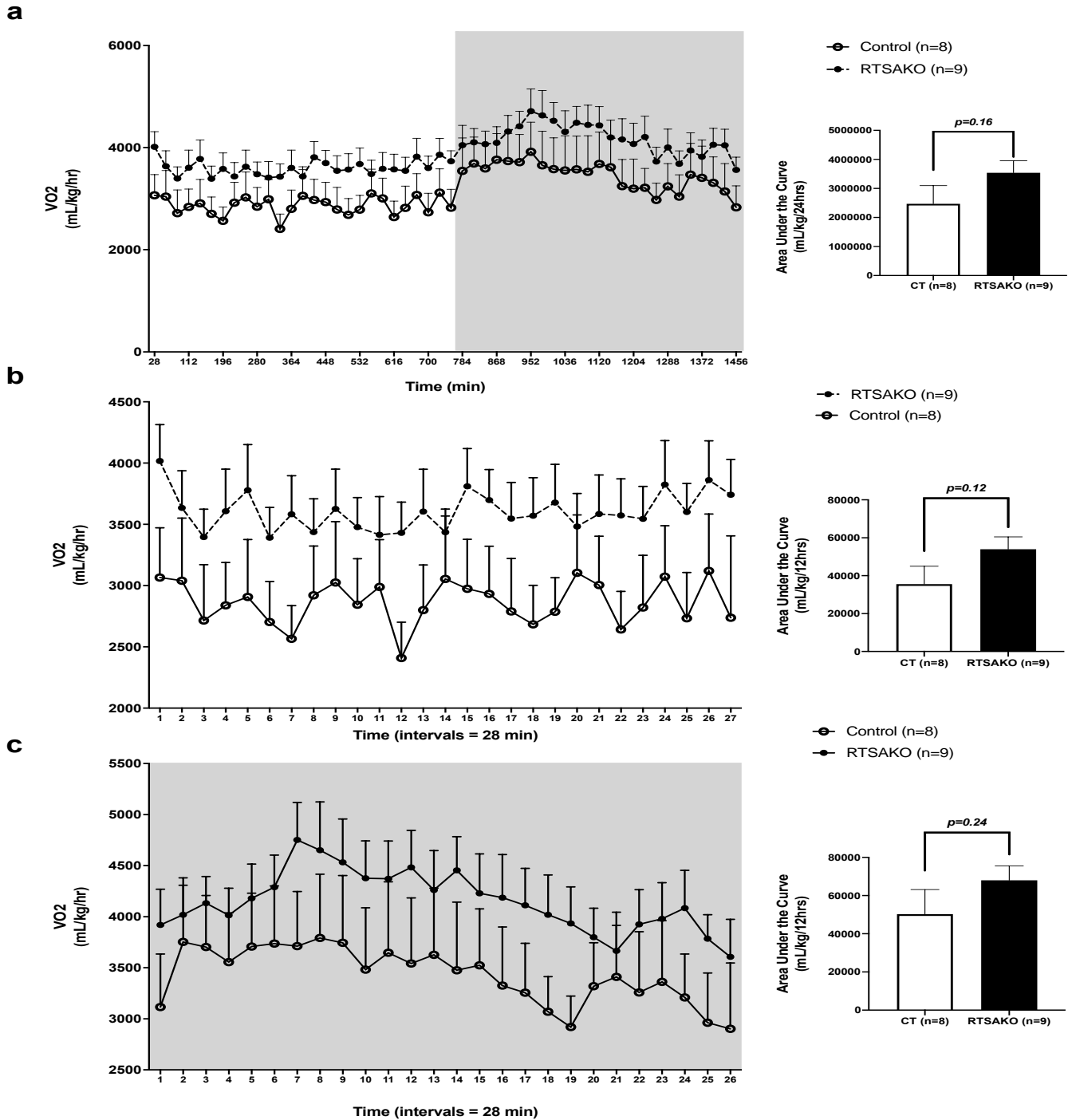


Figure 13: Oxygen consumption rate of Control (CT) and Knockout (RTSAKO) mice
 Fourteen to sixteen-month-old non-fasted RTSAKO and control mice were analyzed in the CLAM system for 24 hours. Activity was measured in 28-minute intervals and during the day (light) and night (dark). a) Total daily VO₂ was analyzed across a 24-hour period, and AUC was calculated across this timespan. b) VO₂ rate was recorded during the light cycle and AUC was calculated during the 12 hours c) VO₂ rate was recorded during the dark cycle and AUC was calculated during the 12 hours.

VCO₂ Testing: The carbon dioxide production of 14-16-month-old female RTSAKO and control mice was analyzed using AUC. In fig.14a, VCO₂ produced by aged female RTSAKO and control littermate mice was assessed, and it was found that there were no significant differences in their overall carbon dioxide production during the 24-hour period, as analyzed by the AUC. As well, carbon dioxide production rate during the light (fig.14b) and dark cycles (fig.14c) was also analyzed by calculating the AUC, and these measures also did not significantly differ between mice with different genotypes.

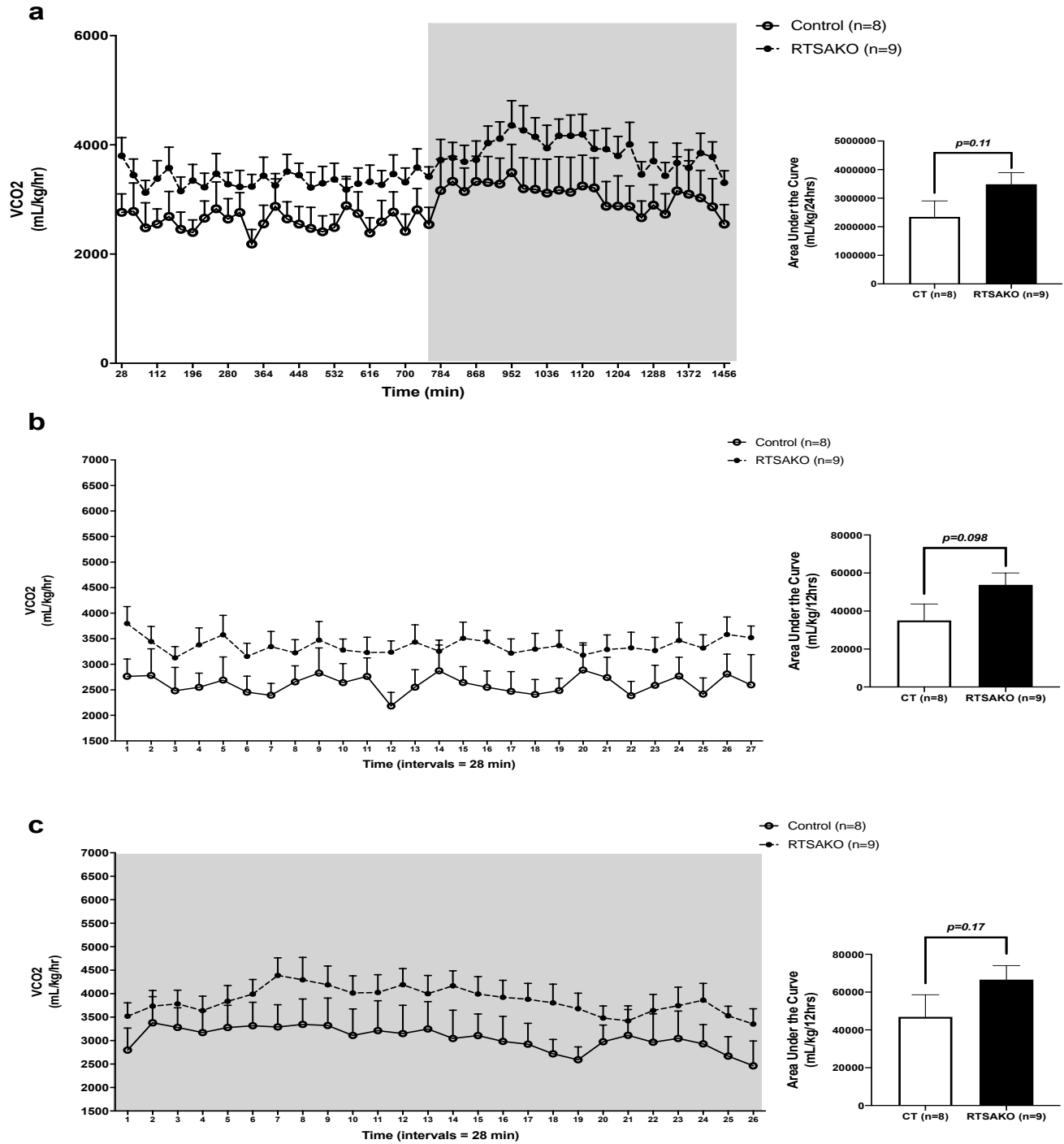


Figure 14: Volume of Carbon Dioxide (VCO₂) in Control (CT) and Knockout (RTSAKO) mice

Fourteen to sixteen-month-old non-fasted female RTSAKO and CT mice were subjected to 24 hours in the CLAM systems. a) VCO₂ activity was measured in 28-minute intervals and during the entire day, and AUC was calculated across this timespan. b) VCO₂ rate was recorded during the light cycle and AUC was calculated during the 12-hour period. c) VCO₂ rate was recorded during the dark cycle was calculated during the 12-hour period.

RER and Heat: RER is a unitless indirect measure, calculated as a ratio of $VCO_2:VO_2$. This value provides a relative measure suggesting the predominate substrate of use. When this value is closer to 1.0, it is an indication that carbohydrates are the major fuel source, whereas an RER closer to 0.7 indicates a greater reliance on fats [109]. In addition, heat measures the energy expended during the 24-hour testing period. Collectively, these measurements are made using a mixture of gases that circulate throughout the chambers and calculations are normalized to the body mass of the subject in kilograms [109]. RER over 24 hours was analyzed using the AUC and there was no significant difference between the RTSAKO mice and their control littermates. Heat was also calculated using AUC, and did not significantly differ between mice with different genotypes.

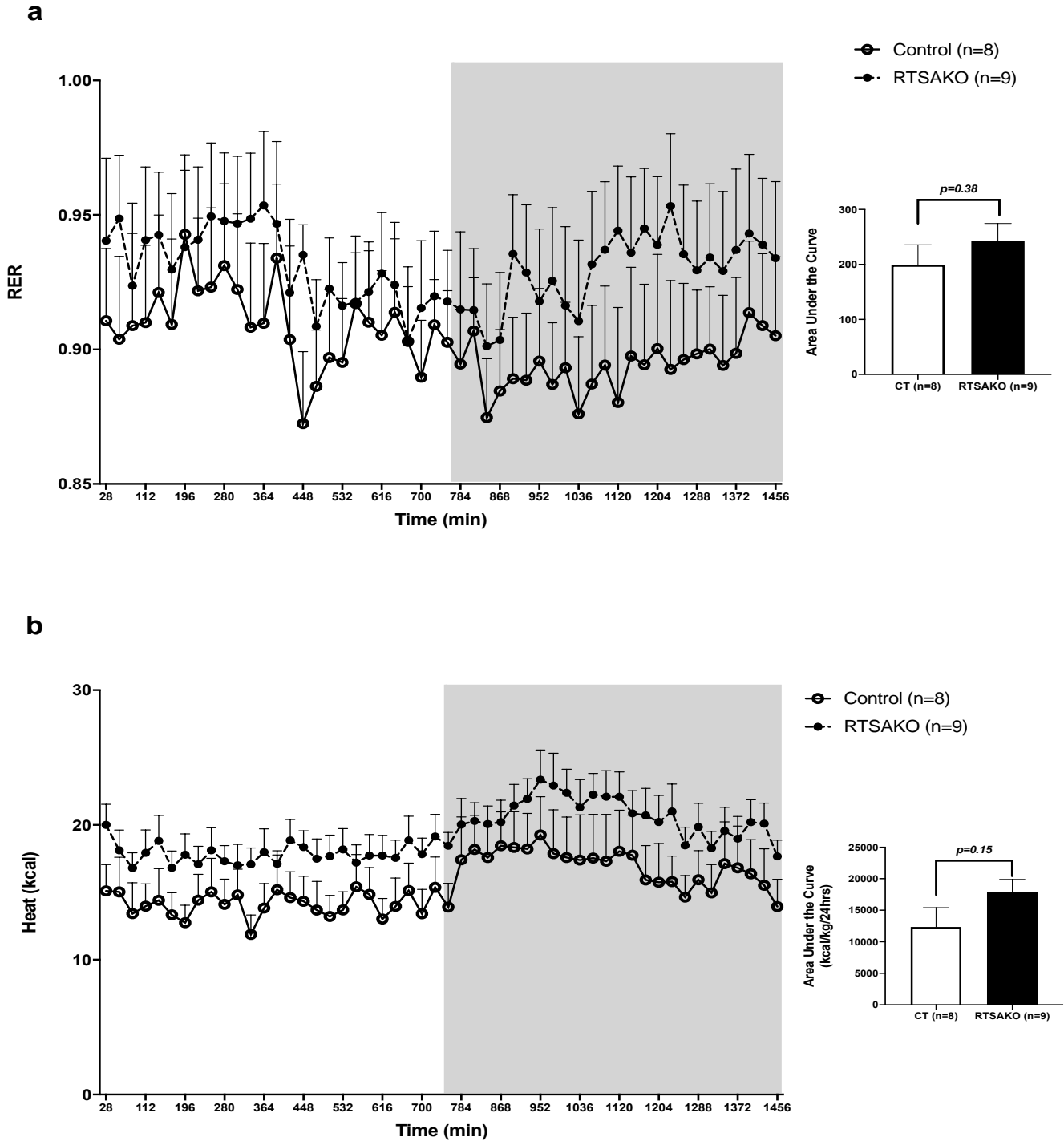


Figure 15: RER and Heat in Control (CT) and Knockout (RTSAKO) mice

Fourteen to sixteen-month-old non-fasted RTSAKO and CT mice were subjected to 24 hours in the CLAM systems. a) Respiratory Exchange Ratio (RER) was measured in 28-minute intervals and during the entire day and AUC was calculated across this timespan. b) Heat was also measured in 28-minute intervals and during the entire day and AUC was calculated across this timespan.

Discussion: The aim of this study was to investigate four metabolic variables in addition to the activity pattern of the 14-16-month-old female RTSAKO mice and their littermate controls during a 24-hour period. Aged female RTSAKO mice have a non-functional ATGL enzyme in the epithelial cells of the proximal and distal renal tubules and are glucose intolerant. To date, the Lipid Enzyme Discovery lab has not studied activity, VO_2 , VCO_2 , RER or heat in the female RTSAKO mice. Therefore, this work was expected to yield new insight into whole-body changes occurring in this model.

Activity in its many forms, ranging from a brisk walk to intense exercising, is recognized as helping to prevent many known metabolic diseases [110]. In the 14-16-month-old female RTSAKO and CT mice, activity was measured in multiple directions. However, differences between RTSAKO and control littermates in activity recorded in all directions: total, ambulatory and rearing, during the 24-hour testing period, does not reach statistical significance. Therefore, there are no differences in overall movement and changes in their grooming patterns in comparison to their control littermates. However, there is a *general* decrease in total and dark locomotor, ambulatory and rearing activity in the aged female RTSAKO mice. Although such observations are not significant, this may indicate that these mice are less active or may groom less in comparison to their control littermates during the nighttime, and over the 24-hour period. Interestingly, such differences are primarily observed during the “dark” or nighttime rather than the “light” or daytime because mice are nocturnal in nature and are known to be most active during the dark time [104]. Interestingly, the p-values for several activity patterns were close to achieving significance. Therefore, an increase in sample size is needed to more definitely conclude whether differences in activity between the 14-16-month-old female RTSAKO mice and their littermate controls exist, or not.

Oxygen consumption and carbon dioxide production are fundamental processes that indicate tissue and organ function [111]. In the 14-16-month-old female RTSAKO mice, disturbances to renal lipid metabolism were not expected to change VO_2 and VCO_2 , since the kidney is only known to use 10 – 15% of oxygen [105]. It was expected that there would be no difference, and as predicted no statistical difference was found, but the statistical analysis of AUC suggested that some of the measures may have been underpowered.

RER, which is a ratio of VCO_2 and VO_2 , is not significantly different in the aged female RTSAKO mice. Although an RER of closer to 1 was expected due to the glucose intolerance in the 14-16-month-old female RTSAKO, there was no difference between both groups of mice as to their preferred source of substrate. Interestingly, the RTSAKO mice and their littermate controls demonstrate a range of RER between 0.86 – 1.0, indicating a preference toward carbohydrate by both groups. However, increasing sample size may aid in better elucidating the data. In addition, energy expenditure, which is expressed as heat in kilocalories, is not significantly different between the 14-16-month-old RTSAKO mice and their littermate controls. Since multiple factors are known to affect energy expenditure, including body composition, physical activity and disease state, it is plausible for the RTSAKO mice to have higher heat production [112], although such observations are absent in the results.

Chapter 6: Integrated Conclusion

This thesis contains studies characterizing the metabolic and physiological differences evident in female RTSAKO mice at 14-16-months of age relative to their littermate controls. In humans, women have a longer latency in disease development, by approximately 10 years versus men [26]. At the time of my joining, other members of our laboratory had characterized male RTSAKO mice at various ages and glucose intolerance was found in 16-18-week-old male RTSAKO mice. As well, female mice up to 6 months of age were analyzed and found to have no changes in glycemic control. Therefore, my thesis focused on examining an aged timepoint, where the female RTSAKO were expected to be more susceptible to the effects of prolonged renal lipid overstorage, but would not yet be severely affected by frailty and complications associated with extreme old age.

The aged female RTSAKO mice were validated as a likely model of isolated renal steatosis, since the expression of *Cre*-recombinase was found to be exclusive to the kidneys, and only renal weights were increased, which we expect was due to TAG over-accumulation, and which we also expect will be directly confirmed in planned future studies. In addition, there was no evidence of lipotoxicity, inflammation or fibrosis although minor elevations in expression of a gene marker of proliferation existed, and could be attributed to the actions of renal stem cells [96]. Most notably, the 14-16-month-old female RTSAKO mice were glucose intolerant and insulin sensitive, indicating that impairments to glycemic control develop with age, signifying a sexual dimorphism. Comparable to the male mice, evidence suggested that renal steatosis affects insulin secretion, and not signaling, in the aged female mice. Treatment with Ki16425 rescued the glucose intolerance, indicating that LPA has a likely causal role in impairing insulin secretion in these mice. Although prior studies have credited Ki16425 treatment for increasing the number

of islet cells in the rescue of insulin levels suppressed by LPA, it is unclear if this is a direct or indirect result. Elucidation of mechanisms underlying the link between LPA and impaired insulin secretion is of current interest [55].

Interestingly, this thesis indicates that with age, the female RTSAKO mice recapitulate the phenotype of the younger male RTSAKO mice. Prior studies by our laboratory have found that females up to 6 month of age are more insulin sensitive than their littermate controls, and the current work in the 14-16-month-old cohort shows that these groups have comparable insulin sensitivity. Therefore, like the males, the females are not insulin resistant. Rather, it is more likely that the older females, also like the males, have impaired insulin secretion. Further studies, including blood collection for insulin analysis immediately following injection of glucose, are required to confirm that insulin secretion is, indeed, impaired in aged female RTSAKO mice. Additionally, more work is needed to understand the mechanism underlying the effects of LPA on insulin secretion in any mouse group.

Analysis of activity and energy expenditure in the aged female RTSAKO mice indicated no significant difference in comparison to the littermate controls. Despite the lack of significance, the results present interesting observations. Food intake, VO_2 , VCO_2 and heat was slightly higher in the RTSAKO mice in comparison to the littermate controls. Interestingly in chapter 3 of this thesis, gene expression of *Pcna* was significantly higher and this alluded to activation of renal repair mechanisms. At the molecular level, tissue repair has a higher energy demand, which results in increases in oxidative metabolism that may increase oxygen requirements [113]. The aged female RTSAKO mice might be consuming more oxygen for kidney repair and healing . However, this is only a speculation and, given the minor effect on the gene expression observed, coupled with the minor role of the kidneys in whole body energy

metabolism, is not highly plausible. Further investigation is needed to understand the apparent increase in energy use, especially if the decrease in activity levels is confirmed in a study with sufficient power.

Although not statistically significant, the RER appeared to be slightly higher in the aged female RTSAKO mice, although both groups of mice had RER values that suggested a greater utilization of carbohydrates compared to fat. With lower circulating insulin, blood glucose uptake by muscle may be low, and this may allow slightly greater access of this substrate to multiple organs of the body, therefore causing RER to be closer to 1 than 0.70 in the female RTSAO mice in comparison to the littermate controls. In order to better understand the preferred substrate of use by both groups of mice, a fasting challenge could be performed, whereby mice are fasted during the duration of the CLAMS study spanning either 12-24 hours. Without food, the mice are obligated to use internal fuel sources, which may aid in elucidating if metabolic differences in fuel usage between the RTSAKO mice and control littermates exist. Overall, the studies on activity and energy metabolism require an increased sample size analysis before conclusions can be made.

Other models of ectopic lipid accumulation exist. However, unlike the RTSAKO mouse model, they are either diet-induced, whole body knockouts or tissue specific knockouts of other organs, which may cause confounding and prevent the tissue-specific understanding of the understudied kidney [22]. In diet-induced models, mice are often fed a high fat diet for weeks or months resulting in an obese-like state [114]. Over time, these mice develop hyperglycemia, hyperinsulinemia, and eventually present with insulin resistance accounting for high blood glucose levels preceding a glucose challenge [114]. As well, obese mice have also been shown to have islet dysfunction [114]. Although these mice have renal steatosis, like the RTSAKO mice

are predicted to have, the global changes in organ ectopic lipid storage and adiposity contribute to a very different phenotype, with evidence of renal fibrosis and inflammation in these animals [115, 116].

Global ATGL deficient mice (*Pnpla2*^{-/-}) show significant increases in TAG accumulation in virtually all tissues, including a 2-fold increase in liver, 3-fold increase in skeletal muscle, 4-fold increase in pancreas and a 15-fold increase in the kidney, but have improved glycemic control [117]. That improvement is attributed to improved tissue glucose use resulting from reduced competition with FFA for oxidation, since impaired adipose tissue lipolysis results in a reduction in circulating NEFA [117]. Unlike RTSAKO mice, *Pnpla2*^{-/-} mice have decreased energy expenditure, reduced VO₂, and impaired thermal regulation [117]. In the global ATGL knockout there are indications of renal dysfunction including albuminuria, lipid vacuolation of the proximal convoluted tubules, tubulointerstitial fibrosis, and a decrease in the creatine clearance rate [116]. PPAR α , a transcription factor involved in fatty acid transport, oxidation and catabolism, is down-regulated in these mice as a result of disruptions to mitochondrial oxidation and respiration, further suggesting suppressed lipid metabolism [116]. Thus, unlike the RTSAKO mice, the *Pnpla2*^{-/-} mice have renal lipotoxicity as evidenced by an overload of renal reactive oxygen species in addition to the TAG accumulation and fibrosis [115]. By 9-10 weeks of age, the *Pnpla2*^{-/-} mice are comparable to individuals with glomerulopathy, where there is dysfunction to the glomerular filtration barrier apart from the significant presence of albuminuria [115]. Such changes are attributed to podocyte injury and apoptosis, which Chen *et al.* confirmed through transmission electron microscopy (TEM), where morphological changes to podocyte mitochondria were observed [115]. Additionally, *Pnpla2*^{-/-} mice are affected by cardiac

complications that are so severe that it causes premature mortality, beginning at just a few months of age [115].

It is unclear why the RTSAKO mice differ so dramatically from the *Pnpla2*^{-/-} mice. One reason may be differences in the extent of renal tubule fat accumulation. In young male RTSAKO mice, kidney TAG increases approximately 2-fold in accumulation, compared with a 15-fold total increase in *Pnpla2*^{-/-} mice [117]. It is also possible that the structures affected, rather than the total fat content *per se*, may be an important factor in determining whether renal pathology develops. For example, other kidney cells and structures, such as podocytes of the glomeruli, may be more susceptible to lipotoxicity, which could precipitate the fibrosis and inflammation observed in *Pnpla2*^{-/-} mice [115, 116]. The dramatic differences in renal pathology between the global *Atgl*-knockout mice and our RTSAKO mice, highlights the importance of a targeted model in understanding the role of ectopic renal tubule TAG accumulation in renal and whole-body physiology and pathophysiology.

In tissue-specific *Pnpla2* knockouts, a variety of phenotypes have been observed. These include liver-, adipose-, heart-, skeletal muscle- and pancreas-specific ATGL knockouts, [117]. Skeletal muscle-specific ATGL knockouts have been shown to have increased glucose uptake and improved insulin sensitivity due to decreased FFA levels [117]. In liver-specific ATGL knockouts, hepatic steatosis developed overtime, and with age, TAG accumulation was exacerbated with no changes to body weight [117]. Unlike, global and adipose-specific *Atgl* knockouts, ATGL was shown to be necessary for hepatic insulin sensitivity [117]. The absence of ATGL in specific organs can affect whole body metabolism in different manners. However, these studies have not reported on kidney health and function as a result of tissue-specific TAG

accumulation. Therefore the role of kidney ATGL on metabolism must be continually studied using the RTSAKO model.

This thesis, which examines older female mice in a kidney-specific ATGL knockout mouse model, has presented interesting findings that both coincide and differ from other studies. Similar to the *Atgl* liver-specific knockouts, the RTSAKO mice show evidence developing steatosis in the gene-targeted organ with age, but do not have changes to body weight. However, our RTSAKO mice are glucose intolerant, but insulin sensitive, like the liver-specific knockouts. Unlike other studies that have only reported on glucose intolerance caused by TAG accumulation due to ATGL deficiency, we were able show the glucose intolerance was likely due to impairments in insulin secretion and not insulin signaling, due to the proposed actions of LPA, whose actions were negated using an LPA receptor blockade. In addition, aged female RTSAKO mice do not develop lipotoxicity although prolonged lipid accumulation is known to result in inflammation in other models [3, 16, 39, 115-117]. Since *Hsl* is not upregulated, at least at the level of gene expression, an excess of DAG and other complex lipids known to cause inflammatory responses and impairments to insulin signaling maybe absent. Further work is required to verify this.

This thesis has several limitations. In order to further validate the importance of LPA in female RTSAKO mice, its concentration in plasma and kidney homogenates should be measured using mass spectrophotometry; presently this resource is unavailable. In addition, studies should repeat glucose tolerance testing with the vehicle control to allow comparison of mice treated with Ki16425 with mice treated with vehicle, which may affect the response. In addition, although it was speculated that increased kidney weights are due to the build-up of TAG, a renal lipid profile should be completed to quantify TAG content in the kidneys of the 14-16-month-old

female RTSAKO mice. Although the expression of various genes was measured, in some cases, further measures of protein level are important. HSL undergoes post-translational modification, and as a result, gene expression may not directly translate into protein expression, and also does not demonstrate modifications to the protein that can affect activity [77]. Therefore, western blotting should be used to accurately confirm expression and post-translational modifications in the aged female mice. In addition, CLAMS should be completed with a larger sample size to determine whether differences exist, since many of the results have a p-value close to 0.05.

Future directions from this thesis lie in completing the above mention experiments, but also further exploring the mechanisms by which LPA affects insulin secretion. LPA is a key signaling molecule implicated in the metabolic changes observed, therefore, knowing how it is synthesized, and its concentration, will be insightful in further understanding the physiology of the aged female RTSAKO mice. This thesis has provided information relevant for understanding the isolated effects of renal steatosis on kidney health and glucose metabolism, which has been poorly understood.

References

1. Hruby A, Hu FB. The Epidemiology of Obesity: A Big Picture. *Pharmacoeconomics*. 2015;33(7):673-89.
2. Ofei F. Obesity - a preventable disease. *Ghana Med J*. 2005;39(3):98-101.
3. Van Herpen NA, Schrauwen-Hinderling VB. Lipid accumulation in non-adipose tissue and lipotoxicity. 2008;94(2):231-41.
4. Mitchell NS, Catenacci VA, Wyatt HR, Hill JO. Obesity: Overview of an Epidemic. 2011;34(4):717-32.
5. Algoblan A, Alalfi M, Khan M. Mechanism linking diabetes mellitus and obesity. *Diabetes, Metabolic Syndrome and Obesity: Targets and Therapy*. 2014:587.
6. Kharroubi AT, Darwish HM. Diabetes mellitus: The epidemic of the century. *World J Diabetes*. 2015;6(6):850-67.
7. Subramanian S, Baidal D, Skyler JS, Hirsch IB. The Management of Type 1 Diabetes. In: Feingold KR, Anawalt B, Boyce A, Chrousos G, Dungan K, Grossman A, et al., editors. *Endotext*. South Dartmouth (MA)2000.
8. Reusch JE, Manson JE. Management of Type 2 Diabetes in 2017: Getting to Goal. *JAMA*. 2017;317(10):1015-6.
9. Nichols CG, Remedi MS. The diabetic beta-cell: hyperstimulated vs. hyperexcited. *Diabetes Obes Metab*. 2012;14 Suppl 3:129-35.
10. Cernea S, Dobreanu M. Diabetes and beta cell function: from mechanisms to evaluation and clinical implications. *Biochem Med (Zagreb)*. 2013;23(3):266-80.
11. Hardy OT, Czech MP, Corvera S. What causes the insulin resistance underlying obesity? *Curr Opin Endocrinol Diabetes Obes*. 2012;19(2):81-7.
12. Kahn SE, Hull RL, Utzschneider KM. Mechanisms linking obesity to insulin resistance and type 2 diabetes. *Nature*. 2006;444(7121):840-6.
13. Ye J. Mechanisms of insulin resistance in obesity. *Front Med*. 2013;7(1):14-24.
14. Longo M, Zatterale F, Naderi J, Parrillo L, Formisano P, Raciti GA, et al. Adipose Tissue Dysfunction as Determinant of Obesity-Associated Metabolic Complications. *Int J Mol Sci*. 2019;20(9).
15. Snel M, Jonker JT, Schoones J, Lamb H, de Roos A, Pijl H, et al. Ectopic fat and insulin resistance: pathophysiology and effect of diet and lifestyle interventions. *Int J Endocrinol*. 2012;2012:983814.
16. Bobulescu IA. Renal lipid metabolism and lipotoxicity. *Curr Opin Nephrol Hypertens*. 2010;19(4):393-402.
17. Olson AL. Regulation of GLUT4 and Insulin-Dependent Glucose Flux. *ISRN Mol Biol*. 2012;2012:856987.
18. Triplitt CL. Understanding the kidneys' role in blood glucose regulation. *Am J Manag Care*. 2012;18(1 Suppl):S11-6.

19. Alsahli M, Gerich JE. Renal glucose metabolism in normal physiological conditions and in diabetes. *Diabetes Res Clin Pract.* 2017;133:1-9.
20. DeFronzo RA, Davidson JA, Del Prato S. The role of the kidneys in glucose homeostasis: a new path towards normalizing glycaemia. *Diabetes Obes Metab.* 2012;14(1):5-14.
21. Gerich JE. Role of the kidney in normal glucose homeostasis and in the hyperglycaemia of diabetes mellitus: therapeutic implications. *Diabet Med.* 2010;27(2):136-42.
22. Deji N, Kume S, Araki S, Soumura M, Sugimoto T, Isshiki K, et al. Structural and functional changes in the kidneys of high-fat diet-induced obese mice. *Am J Physiol Renal Physiol.* 2009;296(1):F118-26.
23. Schoiswohl G, Schweiger M, Schreiber R, Gorkiewicz G, Preiss-Landl K, Taschler U, et al. Adipose triglyceride lipase plays a key role in the supply of the working muscle with fatty acids. *J Lipid Res.* 2010;51(3):490-9.
24. Haemmerle G, Lass A, Zimmermann R, Gorkiewicz G, Meyer C, Rozman J, et al. Defective lipolysis and altered energy metabolism in mice lacking adipose triglyceride lipase. *Science.* 2006;312(5774):734-7.
25. Regitz-Zagrosek V. Sex and gender differences in health. *Science & Society Series on Sex and Science. EMBO Rep.* 2012;13(7):596-603.
26. Fu Y, Yu Y, Wang S, Kanu JS, You Y, Liu Y, et al. Menopausal Age and Chronic Diseases in Elderly Women: A Cross-Sectional Study in Northeast China. *Int J Environ Res Public Health.* 2016;13(10).
27. Palmisano BT, Zhu L, Eckel RH, Stafford JM. Sex differences in lipid and lipoprotein metabolism. *Mol Metab.* 2018;15:45-55.
28. Arsenault BJ, Pelletier W, Kaiser Y, Perrot N, Couture C, Khaw KT, et al. Association of Long-term Exposure to Elevated Lipoprotein(a) Levels With Parental Life Span, Chronic Disease-Free Survival, and Mortality Risk: A Mendelian Randomization Analysis. *JAMA Netw Open.* 2020;3(2):e200129.
29. Ahmadian M, Duncan RE, Jaworski K, Sarkadi-Nagy E, Sul HS. Triacylglycerol metabolism in adipose tissue. *Future Lipidol.* 2007;2(2):229-37.
30. Lass A, Zimmermann R, Oberer M, Zechner R. Lipolysis - a highly regulated multi-enzyme complex mediates the catabolism of cellular fat stores. *Prog Lipid Res.* 2011;50(1):14-27.
31. Lin M-E, Herr DR, Chun J. Lysophosphatidic acid (LPA) receptors: Signaling properties and disease relevance. *Prostaglandins & Other Lipid Mediators.* 2010;91(3-4):130-8.
32. Sheng X, Yung YC, Chen A, Chun J. Lysophosphatidic acid signalling in development. *Development.* 2015;142(8):1390-5.
33. Kautzky-Willer A, Harreiter J, Pacini G. Sex and Gender Differences in Risk, Pathophysiology and Complications of Type 2 Diabetes Mellitus. *Endocr Rev.* 2016;37(3):278-316.

34. Flurkey K, M. Curren J, Harrison DE. Chapter 20 - Mouse Models in Aging Research. In: Fox JG, Davisson MT, Quimby FW, Barthold SW, Newcomer CE, Smith AL, editors. *The Mouse in Biomedical Research (Second Edition)*. Burlington: Academic Press; 2007. p. 637-72.
35. Ceylan B, Ozerdogan N. Factors affecting age of onset of menopause and determination of quality of life in menopause. *Turk J Obstet Gynecol*. 2015;12(1):43-9.
36. Diaz Brinton R. Minireview: translational animal models of human menopause: challenges and emerging opportunities. *Endocrinology*. 2012;153(8):3571-8.
37. Mazure CM, Jones DP. Twenty years and still counting: including women as participants and studying sex and gender in biomedical research. *BMC Womens Health*. 2015;15:94.
38. Birnbaum MJ. Lipolysis: more than just a lipase. *J Cell Biol*. 2003;161(6):1011-2.
39. Engin AB. *What Is Lipotoxicity?* : Springer International Publishing; 2017. p. 197-220.
40. Jenkins CM, Mancuso DJ, Yan W, Sims HF, Gibson B, Gross RW. Identification, cloning, expression, and purification of three novel human calcium-independent phospholipase A2 family members possessing triacylglycerol lipase and acylglycerol transacylase activities. *J Biol Chem*. 2004;279(47):48968-75.
41. Villena JA, Roy S, Sarkadi-Nagy E, Kim KH, Sul HS. Desnutrin, an adipocyte gene encoding a novel patatin domain-containing protein, is induced by fasting and glucocorticoids: ectopic expression of desnutrin increases triglyceride hydrolysis. *J Biol Chem*. 2004;279(45):47066-75.
42. Eichmann TO, Kumari M, Haas JT, Farese RV, Jr., Zimmermann R, Lass A, et al. Studies on the substrate and stereo/regioselectivity of adipose triglyceride lipase, hormone-sensitive lipase, and diacylglycerol-O-acyltransferases. *J Biol Chem*. 2012;287(49):41446-57.
43. Zimmermann R, Strauss JG, Haemmerle G, Schoiswohl G, Birner-Gruenberger R, Riederer M, et al. Fat mobilization in adipose tissue is promoted by adipose triglyceride lipase. *Science*. 2004;306(5700):1383-6.
44. Morak M, Schmidinger H, Riesenhuber G, Rechberger GN, Kollroser M, Haemmerle G, et al. Adipose triglyceride lipase (ATGL) and hormone-sensitive lipase (HSL) deficiencies affect expression of lipolytic activities in mouse adipose tissues. *Mol Cell Proteomics*. 2012;11(12):1777-89.
45. Kraemer FB, Shen WJ. Hormone-sensitive lipase: control of intracellular tri-(di-)acylglycerol and cholesteryl ester hydrolysis. *J Lipid Res*. 2002;43(10):1585-94.
46. Casida JE, Nomura DK, Vose SC, Fujioka K. Organophosphate-sensitive lipases modulate brain lysophospholipids, ether lipids and endocannabinoids. *Chem Biol Interact*. 2008;175(1-3):355-64.
47. Krintel C, Morgelin M, Logan DT, Holm C. Phosphorylation of hormone-sensitive lipase by protein kinase A in vitro promotes an increase in its hydrophobic surface area. *FEBS J*. 2009;276(17):4752-62.
48. Taschler U, Radner FP, Heier C, Schreiber R, Schweiger M, Schoiswohl G, et al. Monoglyceride lipase deficiency in mice impairs lipolysis and attenuates diet-induced insulin resistance. *J Biol Chem*. 2011;286(20):17467-77.

49. Ye X. Lysophospholipid signaling in the function and pathology of the reproductive system. 2008;14(5):519-36.
50. M'Hiri I, Diaguarachchige De Silva KH, Duncan RE. Relative expression and regulation by short-term fasting of lysophosphatidic acid receptors and autotaxin in white and brown adipose tissue depots. *Lipids*. 2020;55(3):279-84.
51. Imamura F, Horai T, Mukai M, Shinkai K, Sawada M, Akedo H. Induction of in vitro tumor cell invasion of cellular monolayers by lysophosphatidic acid or phospholipase D. *Biochem Biophys Res Commun*. 1993;193(2):497-503.
52. Chen J, Baydoun AR, Xu R, Deng L, Liu X, Zhu W, et al. Lysophosphatidic acid protects mesenchymal stem cells against hypoxia and serum deprivation-induced apoptosis. *Stem Cells*. 2008;26(1):135-45.
53. Renbäck K, Inoue M, Ueda H. Lysophosphatidic acid-induced, pertussis toxin-sensitive nociception through a substance P release from peripheral nerve endings in mice. 1999;270(1):59-61.
54. Riser BL, Denichilo M, Cortes P, Baker C, Grondin JM, Yee J, et al. Regulation of connective tissue growth factor activity in cultured rat mesangial cells and its expression in experimental diabetic glomerulosclerosis. *J Am Soc Nephrol*. 2000;11(1):25-38.
55. Rancoule C, Attane C, Gres S, Fournel A, Dusaulcy R, Bertrand C, et al. Lysophosphatidic acid impairs glucose homeostasis and inhibits insulin secretion in high-fat diet obese mice. *Diabetologia*. 2013;56(6):1394-402.
56. Rancoule C, Dusaulcy R, Treguer K, Gres S, Attane C, Saulnier-Blache JS. Involvement of autotaxin/lysophosphatidic acid signaling in obesity and impaired glucose homeostasis. *Biochimie*. 2014;96:140-3.
57. Rancoule C, Dusaulcy R, Treguer K, Gres S, Guigne C, Quilliot D, et al. Depot-specific regulation of autotaxin with obesity in human adipose tissue. *J Physiol Biochem*. 2012;68(4):635-44.
58. Fu Z, Gilbert ER, Liu D. Regulation of insulin synthesis and secretion and pancreatic Beta-cell dysfunction in diabetes. *Curr Diabetes Rev*. 2013;9(1):25-53.
59. Wilcox G. Insulin and insulin resistance. *Clin Biochem Rev*. 2005;26(2):19-39.
60. Olokoba AB, Obateru OA, Olokoba LB. Type 2 diabetes mellitus: a review of current trends. *Oman Med J*. 2012;27(4):269-73.
61. Rix I, Nexoe-Larsen C, Bergmann NC, Lund A, Knop FK. Glucagon Physiology. In: Feingold KR, Anawalt B, Boyce A, Chrousos G, Dungan K, Grossman A, et al., editors. *Endotext*. South Dartmouth (MA)2000.
62. Scott RV, Bloom SR. Problem or solution: The strange story of glucagon. *Peptides*. 2018;100:36-41.
63. Kelesidis T, Kelesidis I, Chou S, Mantzoros CS. Narrative review: the role of leptin in human physiology: emerging clinical applications. *Ann Intern Med*. 2010;152(2):93-100.
64. Zhou Y, Rui L. Leptin signaling and leptin resistance. *Front Med*. 2013;7(2):207-22.

65. Gruzdeva O, Borodkina D, Uchasova E, Dyleva Y, Barbarash O. Leptin resistance: underlying mechanisms and diagnosis. *Diabetes Metab Syndr Obes.* 2019;12:191-8.
66. Meek TH, Morton GJ. Leptin, diabetes, and the brain. *Indian J Endocrinol Metab.* 2012;16(Suppl 3):S534-42.
67. Jamaluddin MS, Weakley SM, Yao Q, Chen C. Resistin: functional roles and therapeutic considerations for cardiovascular disease. *Br J Pharmacol.* 2012;165(3):622-32.
68. Zhao CW, Gao YH, Song WX, Liu B, Ding L, Dong N, et al. An Update on the Emerging Role of Resistin on the Pathogenesis of Osteoarthritis. *Mediators Inflamm.* 2019;2019:1532164.
69. Ix JH, Sharma K. Mechanisms linking obesity, chronic kidney disease, and fatty liver disease: the roles of fetuin-A, adiponectin, and AMPK. *J Am Soc Nephrol.* 2010;21(3):406-12.
70. Yokoo T, Clark HR, Pedrosa I, Yuan Q, Dimitrov I, Zhang Y, et al. Quantification of renal steatosis in type II diabetes mellitus using dixon-based MRI. *Journal of magnetic resonance imaging : JMRI.* 2016;44(5):1312-9.
71. Boss GR, Seegmiller JE. Age-related physiological changes and their clinical significance. *West J Med.* 1981;135(6):434-40.
72. Kim H, Kim M, Im SK, Fang S. Mouse Cre-LoxP system: general principles to determine tissue-specific roles of target genes. *Lab Anim Res.* 2018;34(4):147-59.
73. Leneuve P, Zaoui R, Monget P, Le Bouc Y, Holzenberger M. Genotyping of Cre-lox mice and detection of tissue-specific recombination by multiplex PCR. *Biotechniques.* 2001;31(5):1156-60, 62.
74. Brooks S, Rigby W. Post-transcriptional regulation of tumor necrosis factor alpha expression. *Arthritis Res Ther.* 2004;6(3):15.
75. Chae M, Jung JY, Bae IH, Kim HJ, Lee TR, Shin DW. Lipin-1 expression is critical for keratinocyte differentiation. *J Lipid Res.* 2016;57(4):563-73.
76. Gluchowski NL, Chitraju C, Picoraro JA, Mejhert N, Pinto S, Xin W, et al. Identification and characterization of a novel DGAT1 missense mutation associated with congenital diarrhea. *J Lipid Res.* 2017;58(6):1230-7.
77. Fortelny N, Overall CM, Pavlidis P, Freue GVC. Can we predict protein from mRNA levels? *Nature.* 2017;547(7664):E19-E20.
78. Ahmadian M, Abbott MJ, Tang T, Hudak CS, Kim Y, Bruss M, et al. Desnutrin/ATGL is regulated by AMPK and is required for a brown adipose phenotype. *Cell Metab.* 2011;13(6):739-48.
79. Peter K. Cre Lox Breeding For Beginners, Part 1 [Website]. The Jackson Laboratory 2011 [Available from: <https://www.jax.org/news-and-insights/jax-blog/2011/september/cre-lox-breeding>].
80. Truett GE, Heeger P, Mynatt RL, Truett AA, Walker JA, Warman ML. Preparation of PCR-quality mouse genomic DNA with hot sodium hydroxide and tris (HotSHOT). *Biotechniques.* 2000;29(1):52, 4.

81. Bradley RM, Marvyn PM, Aristizabal Henao JJ, Mardian EB, George S, Aucoin MG, et al. Acylglycerophosphate acyltransferase 4 (AGPAT4) is a mitochondrial lysophosphatidic acid acyltransferase that regulates brain phosphatidylcholine, phosphatidylethanolamine, and phosphatidylinositol levels. *Biochimica et biophysica acta*. 2015;1851(12):1566-76.
82. Valente V, Teixeira SA, Neder L, Okamoto OK, Oba-Shinjo SM, Marie SK, et al. Selection of suitable housekeeping genes for expression analysis in glioblastoma using quantitative RT-PCR. *Ann Neurosci*. 2014;21(2):62-3.
83. Igarashi P, Shashikant CS, Thomson RB, Whyte DA, Liu-Chen S, Ruddle FH, et al. Ksp-cadherin gene promoter. II. Kidney-specific activity in transgenic mice. *Am J Physiol*. 1999;277(4):F599-610.
84. Schlager G. Kidney weight in mice: strain differences and genetic determination. *J Hered*. 1968;59(3):171-4.
85. Krishna M. Role of special stains in diagnostic liver pathology. *Clinical Liver Disease*. 2013;2(S1):S8-S10.
86. Breil C, Abert Vian M, Zemb T, Kunz W, Chemat F. "Bligh and Dyer" and Folch Methods for Solid-Liquid-Liquid Extraction of Lipids from Microorganisms. Comprehension of Solvation Mechanisms and towards Substitution with Alternative Solvents. *Int J Mol Sci*. 2017;18(4).
87. Laggai S, Simon Y, Ransweiler T, Kiemer AK, Kessler SM. Rapid chromatographic method to decipher distinct alterations in lipid classes in NAFLD/NASH. *World J Hepatol*. 2013;5(10):558-67.
88. Idriss HT, Naismith JH. TNF alpha and the TNF receptor superfamily: structure-function relationship(s). *Microsc Res Tech*. 2000;50(3):184-95.
89. Lopez-Castejon G, Brough D. Understanding the mechanism of IL-1beta secretion. *Cytokine Growth Factor Rev*. 2011;22(4):189-95.
90. Tanaka T, Narazaki M, Kishimoto T. IL-6 in inflammation, immunity, and disease. *Cold Spring Harb Perspect Biol*. 2014;6(10):a016295.
91. Wynn TA, Ramalingam TR. Mechanisms of fibrosis: therapeutic translation for fibrotic disease. *Nat Med*. 2012;18(7):1028-40.
92. Ricard-Blum S. The collagen family. *Cold Spring Harb Perspect Biol*. 2011;3(1):a004978.
93. Ma H-P, Chang H-L, Bamodu OA, Yadav VK, Huang T-Y, Wu ATH, et al. Collagen 1A1 (COL1A1) Is a Reliable Biomarker and Putative Therapeutic Target for Hepatocellular Carcinogenesis and Metastasis. *Cancers (Basel)*. 2019;11(6):786.
94. Sand JMB, Genovese F, Gudmann NS, Karsdal MA. Chapter 4 - Type IV collagen. In: Karsdal MA, editor. *Biochemistry of Collagens, Laminins and Elastin (Second Edition)*: Academic Press; 2019. p. 37-49.
95. To WS, Midwood KS. Plasma and cellular fibronectin: distinct and independent functions during tissue repair. *Fibrogenesis Tissue Repair*. 2011;4:21.

96. Gupta S, Verfaillie C, Chmielewski D, Kren S, Eidman K, Connaire J, et al. Isolation and characterization of kidney-derived stem cells. *J Am Soc Nephrol*. 2006;17(11):3028-40.
97. Andrikopoulos S, Blair AR, Deluca N, Fam BC, Proietto J. Evaluating the glucose tolerance test in mice. *Am J Physiol Endocrinol Metab*. 2008;295(6):E1323-32.
98. Thomas A, Belaidi E, Aron-Wisnewsky J, van der Zon GC, Levy P, Clement K, et al. Hypoxia-inducible factor prolyl hydroxylase 1 (PHD1) deficiency promotes hepatic steatosis and liver-specific insulin resistance in mice. *Sci Rep*. 2016;6:24618.
99. Rad B. Bio-Plex Multiplex System. In: Rad B, editor. *Bio-Plex Assays: Analysentechnik*.
100. Rad B. Multiplex Immunoassay 2020 [Available from: https://www.bio-rad.com/en-ca/applications-technologies/multiplex-immunoassays?source_wt=tech_bio-plex_surl&ID=LUSM0E8UU].
101. Galgani J, Ravussin E. Energy metabolism, fuel selection and body weight regulation. *Int J Obes (Lond)*. 2008;32 Suppl 7:S109-19.
102. Mtaweh H, Tuira L, Floh AA, Parshuram CS. Indirect Calorimetry: History, Technology, and Application. *Front Pediatr*. 2018;6:257.
103. Ramos-Jimenez A, Hernandez-Torres RP, Torres-Duran PV, Romero-Gonzalez J, Mascher D, Posadas-Romero C, et al. The Respiratory Exchange Ratio is Associated with Fitness Indicators Both in Trained and Untrained Men: A Possible Application for People with Reduced Exercise Tolerance. *Clin Med Circ Respirat Pulm Med*. 2008;2:1-9.
104. Bains RS, Wells S, Sillito RR, Armstrong JD, Cater HL, Banks G, et al. Assessing mouse behaviour throughout the light/dark cycle using automated in-cage analysis tools. *J Neurosci Methods*. 2018;300:37-47.
105. Hansell P, Welch WJ, Blantz RC, Palm F. Determinants of kidney oxygen consumption and their relationship to tissue oxygen tension in diabetes and hypertension. *Clin Exp Pharmacol Physiol*. 2013;40(2):123-37.
106. Nie Y, Gavin TP, Kuang S. Measurement of Resting Energy Metabolism in Mice Using Oxymax Open Circuit Indirect Calorimeter. *Bio Protoc*. 2015;5(18):e1602.
107. Laboratories H. Teklad 22/5 Rodent Diet. In: Laboratories H, editor. 2008.
108. Pellizzon M. Choice of laboratory animal diet influences intestinal health. *Lab Animal*. 2016;45(6):238-9.
109. Instruments C. Oxygas for Windows. In: International CI, editor. *User Manual*. Columbus, Ohio 2011. p. 1-75.
110. Montesi L, Moscatiello S, Malavolti M, Marzocchi R, Marchesini G. Physical activity for the prevention and treatment of metabolic disorders. *Intern Emerg Med*. 2013;8(8):655-66.
111. Takala J. Oxygen Consumption and Carbon Dioxide Production: Physiological Basis and Practical Application in Intensive Care. *Anaesthesia, Pain, Intensive Care and Emergency Medicine—APICE*: Springer; 1997. p. 155-62.
112. Psota T, Chen KY. Measuring energy expenditure in clinical populations: rewards and challenges. *Eur J Clin Nutr*. 2013;67(5):436-42.

113. Kimmel HM, Grant A, Ditata J. The Presence of Oxygen in Wound Healing. *Wounds*. 2016;28(8):264-70.
114. Winzell MS, Ahrén B. The High-Fat Diet–Fed Mouse. A Model for Studying Mechanisms and Treatment of Impaired Glucose Tolerance and Type 2 Diabetes. 2004;53(suppl 3):S215-S9.
115. Chen W, Jiang Y, Han J, Hu J, He T, Yan T, et al. Atgl deficiency induces podocyte apoptosis and leads to glomerular filtration barrier damage. *FEBS J*. 2017;284(7):1070-81.
116. Chen W, Zhang Q, Cheng S, Huang J, Diao G, Han J. Atgl gene deletion predisposes to proximal tubule damage by impairing the fatty acid metabolism. *Biochem Biophys Res Commun*. 2017;487(1):160-6.
117. Trites MJ, Clugston RD. The role of adipose triglyceride lipase in lipid and glucose homeostasis: lessons from transgenic mice. *Lipids in Health and Disease*. 2019;18(1):204.